Adaptation to complex environments reveals pervasive trade-offs and genomic targets with large pleiotropic effects

Alexandre Rêgo[1*], Dragan Stajic[1,2], Maria de la Paz Celorio-Mancera[3], Rike Stelkens[1]

[1] Department of Zoology, Stockholm University, Stockholm 114 19, Sweden

[2] Institute for Fish and Wildlife Health, University of Bern, Bern, 3012, Switzerland

[3] Department of Ecology, Environment, and Plant Science , Stockholm University, Stockholm 114 19, Sweden

* Corresponding author: alexandre.rego@ebc.uu.se

Abstract

Populations in nature rarely adapt to a single stress at a time. Various biotic and abiotic factors come together to produce a complex environment to which populations must adapt. How populations adapt to multiple stressors simultaneously, and how trade-offs evolve between these stressors has been of interest to evolutionary biologists for decades. But natural populations often present logistical challenges to understanding the dynamics of evolution and isolating the genetic basis of adaptation. Here we use methods in experimental evolution to test how adaptation proceeds in the presence of co-occurring stressors, and to quantify the evolution of trade-offs between stressors in a complex environment. We adapted populations of the yeast Saccharomyces cerevisiae to a full-factorial combination of four stressors over the course of 15 serial transfers. We observed rapid increases in fitness paired with the accumulation of mutations related to specific stressors. Trade-offs evolved rapidly and dynamics of trade-off evolution varied between stressors, likely due to the inherent physiological and genetic basis of resistance to each stressor. The degree of parallelism at the phenotypic level showed evidence of being modified by the degree of environmental complexity, while parallelism at the genic level was apparent between populations which shared stressors.

Keywords: evolve and resequence; Saccharomyces cerevisiae; complex environments; phenotypic evolution; genomic evolution; stressor interactions; antagonism; synergism; predictability

Introduction

Natural populations usually experience multiple selective pressures at the same time. Habitats are rich with ecological complexity, resulting in many sources of selection through biotic and abiotic factors (Orsini et al., 2012). The dimensionality of concurrent selective pressures has likely even increased for many populations in the Anthropocene due to additional effects of pollution, urbanization, and climate change (Hendry et al., 2017). Predicting the dynamics and outcomes of adaptation to complex environments has been a long-standing goal, with far-reaching implications, e.g. from conservation to the evolution of antimicrobial drug resistance (Hendry et al., 2017; Sommer et al., 2020). Measuring and describing adaptation to complex environments is not trivial given logistical limitations to working with natural populations and the difficulty of assigning causes of selection in nature (Vandenkoornhuyse et al., 2010). Experimental evolution studies are now more often implementing temporally and spatially variable or multidimensional selection regimes as a bridge to investigate evolutionary dynamics in ecologically complex natural environments (Barrett et al., 2005; Kram et al., 2017; Sommer et al., 2020). Even so, few current studies additionally integrate genomic sampling and time-series components to address the underlying genomic basis and dynamics of adaptation to complex environments.

Adaptation to complex environments is consistently marked by the existence of trade-offs (Garland Jr et al., 2022). Theory predicts that a particular phenotype cannot be optimal for all selective pressures, and that most populations exist along a range of phenotypes that optimize fitness in multidimensional selection regimes (Shoval et al., 2012). Trade-offs for multiple traits, through resource limitation, antagonistic pleiotropy, genetic correlations, or epistasis, are common (Roff, 2000; Garland Jr et al., 2022). However, several experimental evolution studies show that populations can improve fitness in many dimensions simultaneously (Bennett & Lenski, 2007; McGee et al., 2016; Bono et al., 2017). Empirical evidence of how trade-offs themselves evolve, and affect dynamics of adaptation over short time scales, is relatively uncommon (Roff & Fairbairn, 2007; Vincent et al., 2013; Bono et al., 2017).

Not only is adaptation in complex environments influenced by the prevalence of trade-offs, but the dynamics of phenotypic (i.e. trait trajectory, rate of fitness changes) and genomic (i.e. rate of allele frequency change, number of SNPs) evolution can also be influenced by the complexity of environments. For example, when multiple stressors simultaneously increase the strength of selection, the trajectory of traits and the rate of fitness changes can be altered (Orr, 2005). Previous microbial work has demonstrated that the rate of adaptation increased with the strength of selection (e.g. Cisneros- Mayoral et al. 2022). Increased selection in more complex environments may also have demographic effects. Reduced population sizes can lead to reduced genetic diversity and mutation availability, as well as increased genetic drift (Ewens, 2004). If the genetic mechanisms underlying adaptation to multiple stressors differ from those governing adaptation to single stressors, distinct adaptive solutions for a particular environmental component may occur between environments of differing compositions (Elena & Lenski, 2003).

The repeatability of adaptation across all biological scales is inevitably influenced by the same parameters that shape adaptation dynamics. However, certain predictions regarding how environmental complexity affects predictability can appear contradictory. For instance, higher selection strengths are expected to enhance repeatability (Orr, 2005), a pattern we might anticipate in complex environments with strong selection pressures. But higher-complexity environments may also exhibit a more polygenic basis for adaptation, which can reduce repeatability due to the greater number of potential evolutionary paths for populations to explore during adaptation (Elmer et al., 2014). These modulators of predictability are further exacerbated when evolving from *de novo* mutations, as the order of mutation can greatly influence future outcomes of adaptation via epistasis and potentiation (Kent & Green, 2017).

Theoretical and empirical results indicate that the shape of trade-offs in complex environments can alter evolutionary trajectories (Bonsall & Mangel, 2004; Lindberg & Collins, 2020). However, while some studies focus on outcomes of adaptation and trade-offs, few do so with time-series data to observe the dynamics of trade-off evolution itself (Huang et al., 2017; Orr et al., 2022). Fewer still incorporate paired phenotypic and

genomic analyses of time-series data to test the basis of adaptation and the potential genetic basis of trade-offs. To understand how the dynamics and outcomes of adaptation differ in complex environments, we performed an evolution experiment with the yeast *Saccharomyces cerevisiae* in which replicate populations of yeast were adapted in four single stressors and full-factorial combinations of the four stressors. We collected phenotypic and genomic time-series data to investigate the dynamics of adaptation. This enabled us to assess the tempo and mode of adaptation, including the trajectory in multidimensional adaptive space that populations explore when concurrent environmental stressors are present. Populations were sampled for both fitness measurements and whole-genome population sequencing (Pool-seq) to look at the dynamics at different biological scales. The fitness of populations evolved in complex environments was measured in both the complex selective media and in media containing only one of each of the individual components, to test for the existence of trade-offs. Our goals were to determine (i) if and how the rate of phenotypic and genomic adaptation depends on the complexity of the environment, (ii) to what extent trade-offs exist and evolve in complex environments, and (iii) whether complex environments produce more or less parallelism.

Methods

Strain information and environments

All strains used in this study were derived from a S288c strain background. The ancestral population was a haploid LJY170 strain (*MATa, hisΔ200, trpΔ63*, donated by Lars Jansen, Oxford University; Stajic, Perfeito, and Jansen 2019). A fluorescent strain RSY328 (*MATa, hisΔ200, trpΔ63, chrV 115940-116010::NatMX6-mCitrine*) was used as an ancestral reference for flow cytometry (see below). RSY328 was constructed by integration of a NatMX6-mCitrine cassette into an intergenic region on chromosome V, creating a deletion of the sequence spanning the positions 115,940bp to 116,010bp without affecting ORFs of neighboring genes. The NatMX6-mCitrine construct was amplified from a pRS5 plasmid, designed by insertion of mCitrine from pFA6a-ACT1-ymCitrineM233I::HISMX6 into a pAG25 backbone using HindIII and BglII restriction enzymes.

Four stressors were used in full-factorial combinations, resulting in a total of 15 environments: 0.8M NaCl (denoted as N), 0.5% Glucose YPD (denoted as S for "starvation"), 37°C (denoted as H for "high heat"), and 20μg/ml of the antifungal Fluconazole (denoted as A for "antifungal") (Fig. 1A). Complex environments are denoted with the combination of abbreviations (e.g. an environment containing salt, antifungal, and high heat is denoted as 'NAH'). Numbers following letter combinations indicate replicates (e.g. NAH1, NAH2, ...). The number of environmental components is designated as the dimensionality of the environment (e.g. single-component environments as '1D', and so on). Populations not grown in heat stress (at 37°C) were grown at a benign 25°C. To quantify the potential selective pressure of each environment, we grew the ancestral population in each environment for 24h from an initial optical density of 0.02 at 600nm (OD600) and measured the reduction in final OD600 relative to the OD600 in the base yeast extract peptone dextrose (YPD; 1% yeast extract, 2% peptone, 2% dextrose) medium at 25°C (Fig. 1B).

Experimental evolution

At the start of experimental evolution for each environment, an individual colony was isolated to serve as the ancestral population, by streaking from frozen stock culture and growing on YPD agar plates (2% agar), for 24 hours. Cells were inoculated in 5ml liquid YPD for 24 hours at 25°C and 200rpm. Then, four replicates were inoculated in 5mL of each environment, serving as biological replicates. Starting population size across all replicates was standardized to OD600 of 0.02 using a BioTek EPOCH2 microplate reader. Cultures were grown in their respective environments at 200 rpm. Every 48 hours 2% (100μl) of the culture was transferred to fresh media. In total, 15 transfers were completed and samples were preserved in 44% glycerol at -80°C for phenotypic and genomic analyses (Fig. 1C). Samples were visually assessed for bacterial or fungal contamination during each transfer under a microscope and, if contamination was present, re-inoculated from the last frozen timepoint.

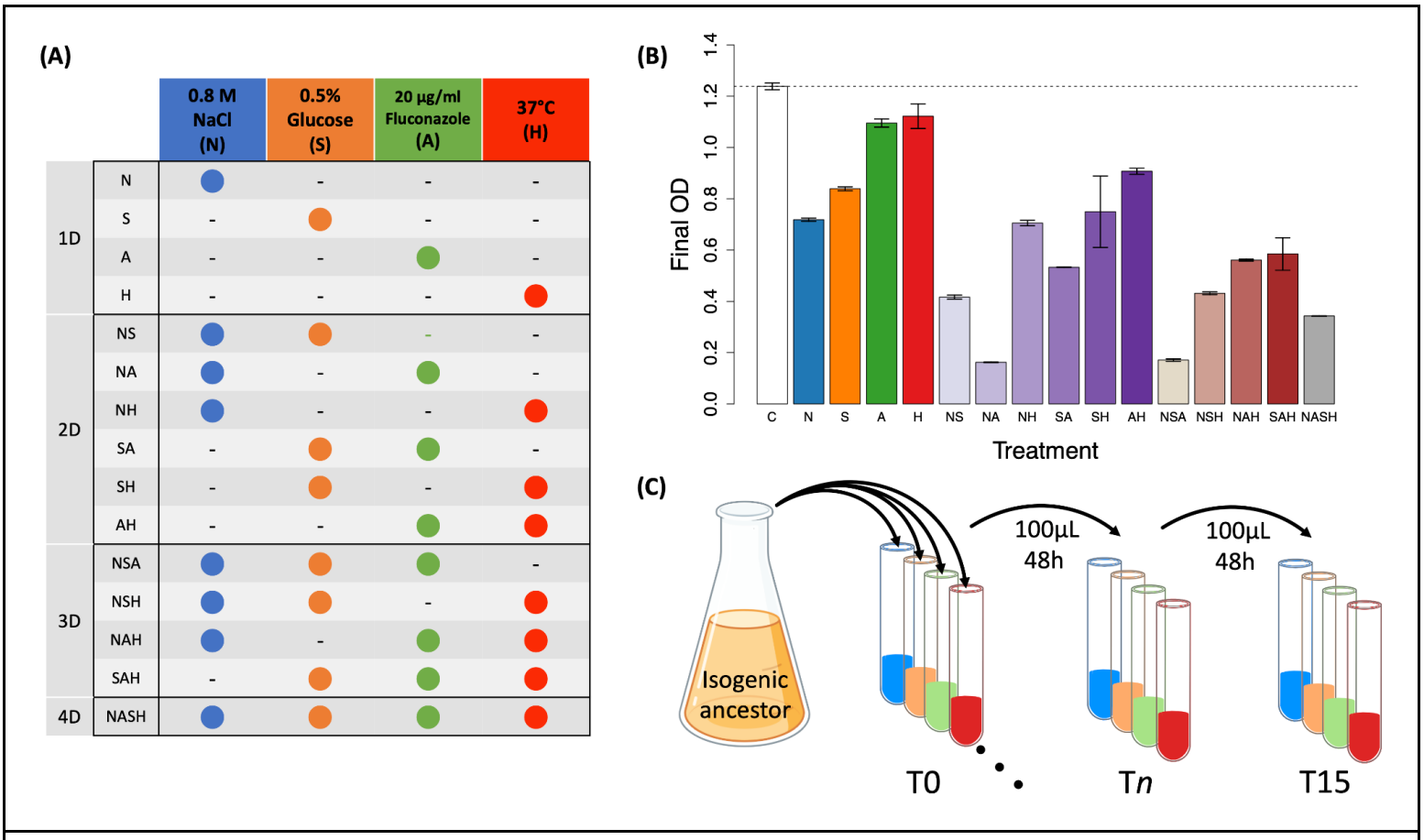

Fig 1. Experimental set-up and stressor effects for each environment. (A) Populations were evolved in every stressor and full-factorial combination of stressors. Colored circles represent the presence of a stressor. Abbreviations are given for each combination of stressors, as well as the 'dimensionality' of the environmental complexity. (B) The stressor effect of each environment in the ancestor was measured as the difference in final OD after 24 hours in a selective environment relative to benign YPD medium. The mean estimate is given and error bars represent the standard error. (C) From an initially isogenic colony, replicate populations of yeast were inoculated into every combination of environments. Populations were then evolved through serial transfer every 48 hours where 2% (100µL) of the culture was transferred into fresh media for a total of 15 transfers. Phenotyping and pooled-sequencing were conducted at T7 and T15.

Fitness assays

Flow cytometry was performed using a Luminex Guava easyCyte. A fluorescently labeled strain (RSY328; MATα, hisΔ200, trpΔ63, chrV 115940-116010::NatMX6- mCitrine) derived from the ancestral genetic background was used as a proxy for the ancestor. The fluorescent strain was streaked on YPD agar and an individual colony was chosen to be inoculated at 25°C and 200 rpm shaking for 24h prior to measurement in the flow-

cytometer. Frozen samples of the evolved populations at transfer 7 (T7) and 15 (T15) were thawed and 100μL was inoculated into 5mL of the population's selective environment for 24 hours. For each evolved population, three technical replicates were tested. After overnight growth, evolved populations were mixed in a 1:1 cell ratio with the fluorescent strain such that the final OD of the mixture was 0.02. Each evolved population was assayed in every single-stressor treatment, including YPD with no additional stressor, as well as in the relevant multi-stressor treatment (if complex). The number of ancestral fluorescent and non-fluorescent evolved cells were measured using flow cytometry after the initial 1:1 mixing (0 hours) and after 48 hours to determine the change in proportion of evolved to ancestral cells. Prior to measurement with flow cytometry, mixed cultures were diluted to an OD of 0.005 and suspended in PBS (7.4pH) solution.

Selection coefficients representing the relative fitness of the evolved strain to the ancestor were calculated as the slope of the linear regression of the log ratio cell numbers ($\frac{evolved}{ancestral}$) on the approximate estimates of generations (cell doublings) between time points (0 hours and 48 hours). Positive coefficients indicate that the evolved population has higher fitness than the ancestor, and *vice versa* for negative coefficients. Each linear regression was run with the three technical replicates per population. Clonal insertion of the fluorescent protein paired with a NAT-resistance selective marker potentially affected the fitness of the ancestral strain in some environments. To account for any fitness effects of the selective marker, we also estimated the selection coefficients between the fluorescent and non-fluorescent ancestor in every environment and subtracted these estimates from the evolved-to-fluorescently marked selection coefficients. Typically selection coefficients estimated from competition assays are used to compare the relative fitness of two individual haplotypes. In our experiment, it is possible that multiple haplotypes existed in a single replicate population, and in such cases the selection coefficient is measuring the mean fitness of a potentially diverse replicate population.

To test for phenotypic parallelism, and whether increased environmental complexity may affect parallelism, we calculated the variance of selection coefficients among replicates for each treatment at T7 and T15. The amount of variance at T7 and T15 among replicates

indicates the degree of parallelism at each time point, and represents the dynamics of parallelism in adaptation to a particular environment. For example, high variance at T7 but low variance at T15 may indicate that populations took alternative adaptive trajectories to reach a similar fitness. We then fit a generalized linear model on the log10 variance to fit model linearity assumptions, and time point as a nested random effect within complexity level. This allows us to estimate the effect environmental complexity has on variance/parallelism at each time point.

Sequencing and bioinformatic processing

To culture cells for sequencing, 100µL of the frozen evolved population were inoculated in 5ml of the evolved population's environment for 24 hours with shaking at 200 rpm. Approximately 1ml of the culture was used for DNA extraction. DNA was extracted from an individual colony of the ancestral stock population and whole population samples at T7 and T15 of experimental evolution. The isolation of gDNA was conducted either by using a column-based method following manufacturer's instructions (NucleoSpin Microbial DNA kit, Macherey-Nagel, Du¨ren, Germany) or an automated system (King Fisher Duo Prime System, Thermo Scientific, MA, USA) in combination with a magnetic bead-based method (Mag-Bind Blood & Tissue DNA HDQ kit, Omega Bio-Tek, GA, USA). Quantification of gDNA samples was conducted using a fluorometric method (Qubit, Thermo Scientific, MA, USA) and library preparation was conducted either in the laboratory or at the National Genomics Infrastructure Sweden (NGI). For the Anc, A1/A2, and AH1/AH2 samples, the libraries were prepared using a DNA Prep Tagmentation kit and IDT (UD) indexes (Illumina, Hayward, CA, USA). The libraries were sequenced at the NGI on an Illumina MiniSeq platform with a 2x150 bp paired-end setup using a MiniSeq Mid Output kit. All other samples were prepared using an DNA Flex library kit (Illumina, Hayward,CA, USA) and sequenced on an Illumina NovaSeq6000. Estimated average genome-wide coverage per sample ranged from 37.29–416.66x. Sequence data are submitted to ENA, accession number XXX.

The quality of sequencing reads after trimming with Trimmomatic v0.36 were assessed with FastQC v0.11.9 and MultiQC v1.11. The reference strain used was S288c (R64, GCF

000146045.2). Reads were aligned using BWA MEM v0.7.17 with the following parameters: -k 20 -r 1.3 -M. Reads were sorted and merged with samtools v1.17 (Danecek et al., 2021), and deduplicated with Picard v2.23.4 (Broad Institute). To call variants, we used GATK v4.1.4.1 HaplotypeCaller best practices (McKenna et al., 2010). The raw VCF was filtered with the following criteria: QD < 0.5, QUAL < 20. Regions of the genome which were not uniquely mapping to itself were then filtered out using GenMap v2.4.1 (K31, E2) (Pockrandt et al., 2020), retaining 3070 variants. Sites were further filtered out if variants existed in the ancestral population, existed at <5% frequency in all populations and time-points (non-informative), had less than 20 reads in greater than 20% of the total samples, had more than 10% of samples missing data, or were found in more than 10% of samples (systematic bad calls). After filtering, 1048 variants remained. We then manually inspected mapped reads of each of the 736 SNPs and 172 INDELs individually in the Integrative Genome Viewer v2.16.0. Sites mapping to multiple locations, variant caller inconsistencies, and homopolymeric or tandem repeat regions were discarded, resulting in a final set of 228 SNPs and 57 INDELs. Allele frequencies were calculated using the ratio between alternate and total allele depth. For each mutation, we estimated its putative effect size using snpEff (Cingolani et al., 2012), which uses the annotation of our reference strain to predict functional effects based on the type of mutation observed (e.g. synonymous, missense, frame-shift, etc).

Copy number variation

We assessed potential partial- and whole-chromosome copy number variations (CNVs). For partial CNVs, we calculated relative depth per sample across 5kb non-overlapping windows compared to mean depth for each chromosome individually. Sites which differed by more than 20% of the mean relative depth per chromosome in the ancestral sample were excluded for analyses as likely repetitive regions which skew results based on mean depth. Some samples had non-uniform read depth across chromosomes, where the centers of chromosomes had lower depth than the ends, leading to a wide U-shape pattern. This is a common pattern described in previous work, but is not associated with average sample coverage, flow-cell, or sequencing machine (Abbey et al., 2014; Ament-Velásquez et al.,

2022; Sun et al., 2023). Similarly to Abbey et al. (2014), for every sample we fit a LOWESS curve for each chromosome based on relative depth by distance-to-chromosome-end. Relative depths were divided by the output of the LOWESS function to normalize this U-shaped pattern in the data. To detect whole-chromosome aneuploidies, which are not dependent on uneven depth across chromosomes, we calculated relative mean depth per chromosome compared to the mean whole-genome read depth. We identified putative CNVs as windows or chromosomes which had a change in relative depth of greater than 20% from the Ancestor (Bendixsen et al. 2021) to either subsequent time point (T7 or T15).

Results

Fitness dynamics

To quantify the selective pressure of each environment, and the combination of components, we grew the ancestral population in each of the 15 environments for 24h from an initial optical density (OD600) of 0.02 and measured the reduction in final OD600 ($\Delta OD = OD_{YPD} - OD_{Selected}$, Mean±SE) relative to the OD600 in YPD at 25°C (OD600 = 1.238±0.013). Of the 1D environments, the salt (ΔOD = -0.520±0.006) and starvation environments (ΔOD = -0.399±0.008) had the largest stressor effects, while antifungal (ΔOD = -0.143±0.159) and heat (ΔOD = -0.116±0.048) had more moderate effects (Fig. 1B).

Because fitness in serial transfer experiments is integrated over several phases of growth (i.e. lag, fermentation, respiration, and stationary phases), we do not use final OD as a measure of adaptation, but only as an estimate of the stressor effect. Instead, to determine how much a population has adapted, we measure the fitness of evolved populations relative to the fitness of the ancestral population in growth competition assays (Gordo, Perfeito, and Sousa 2011). Almost all populations show evidence of adaptation at the midpoint of experimental evolution (T7), except for H1, all four replicates of SH, and NASH1 (Fig. 2). The largest selection coefficient at the midpoint was observed in A2 (S=0.468), with SA populations having the highest selection coefficients on average ($\underline{S}_{SA}$=0.431, SE=0.007). By the endpoint of experimental evolution (T15), populations

tended to increase or seemingly plateau in fitness. Of the 1D populations, only populations adapting to salt showed continued adaptation. Within the first 7 transfers, the mean magnitude of adaptation increased as complexity increased ($\underline{S}_{1D}$=0.177, SE=0.038; $\underline{S}_{2D}$=0.219, SE=0.031; $\underline{S}_{3D}$=0.219, SE=0.029; $\underline{S}_{4D}$=0.238, SE=0.026). Between T7 and T15, the largest increase in adaptation on average was again seen in higher complexity environments (3D and 4D), indicating that lower-complexity environments tended to, at least temporarily, plateau in fitness ($\Delta\underline{S}_{1D}$=0.024, SE=0.029; $\Delta\underline{S}_{2D}$=0.024, SE=0.014; $\Delta\underline{S}_{3D}$=0.085, SE=0.014; $\Delta\underline{S}_{4D}$=0.063,SE=0.040).

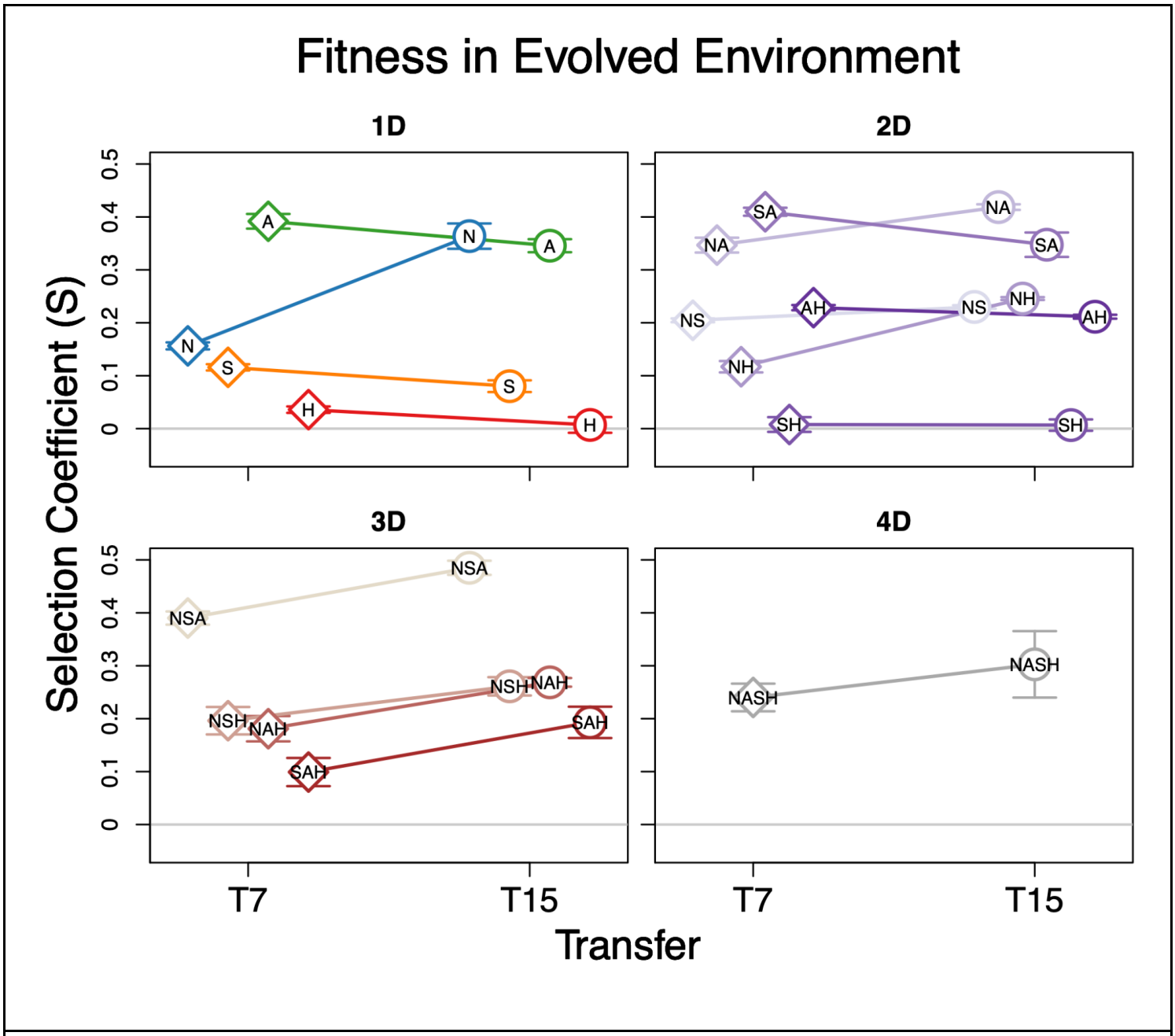

Fig 2. Selection coefficients at T7 and T15 for each environment, partitioned by environmental complexity level (1D–4D). Mean selection coefficients of the four replicates for each treatment are given as points and bars represent the standard deviations. T0 is excluded for visualization purposes, as all points at T0 would fall on the zero-line.

Cost of Adaptation and Evolution of Trade-offs

We measured and quantified the existence of potential trade-offs during evolution in three contexts: trade-offs in (1) the 'ancestral' YPD environment, (2) stressors not experienced during experimental evolution, and (3) adaptations to each component comprising respective complex environments. For context 1, we estimated the selection coefficient of each population tested in YPD. For context 2, we estimated the selection coefficient of each population in every environment that it was not evolved in. In both (1) and (2), reduced fitness in YPD or non-selected environments, respectively, would indicate the existence of trade-offs for those environments. For context 3, we assessed the fitness of ≥2D populations in each respective individual component against populations exclusively evolved to each component. Reduced fitness of ≥2D populations in one or more individual components compared to 1D populations would suggest the presence of trade-offs between adaptations to those components.

Context 1: We first tested the cost of adaptation to the ancestral YPD environment at each time point by measuring the selection coefficient in YPD for each evolved population at both time points (S_{Anc_Tn}). Across all treatments and replicates, there was initially an average maladaptation for the ancestral environment at T7 ($\underline{S}_{Anc_T7}$ = -0.022, SD= 0.13) that were compensated for by T15 ($\underline{S}_{Anc_T15}$ = 0.013, SD=0.066; paired t=-2.62, p=0.011) (Fig. 3).

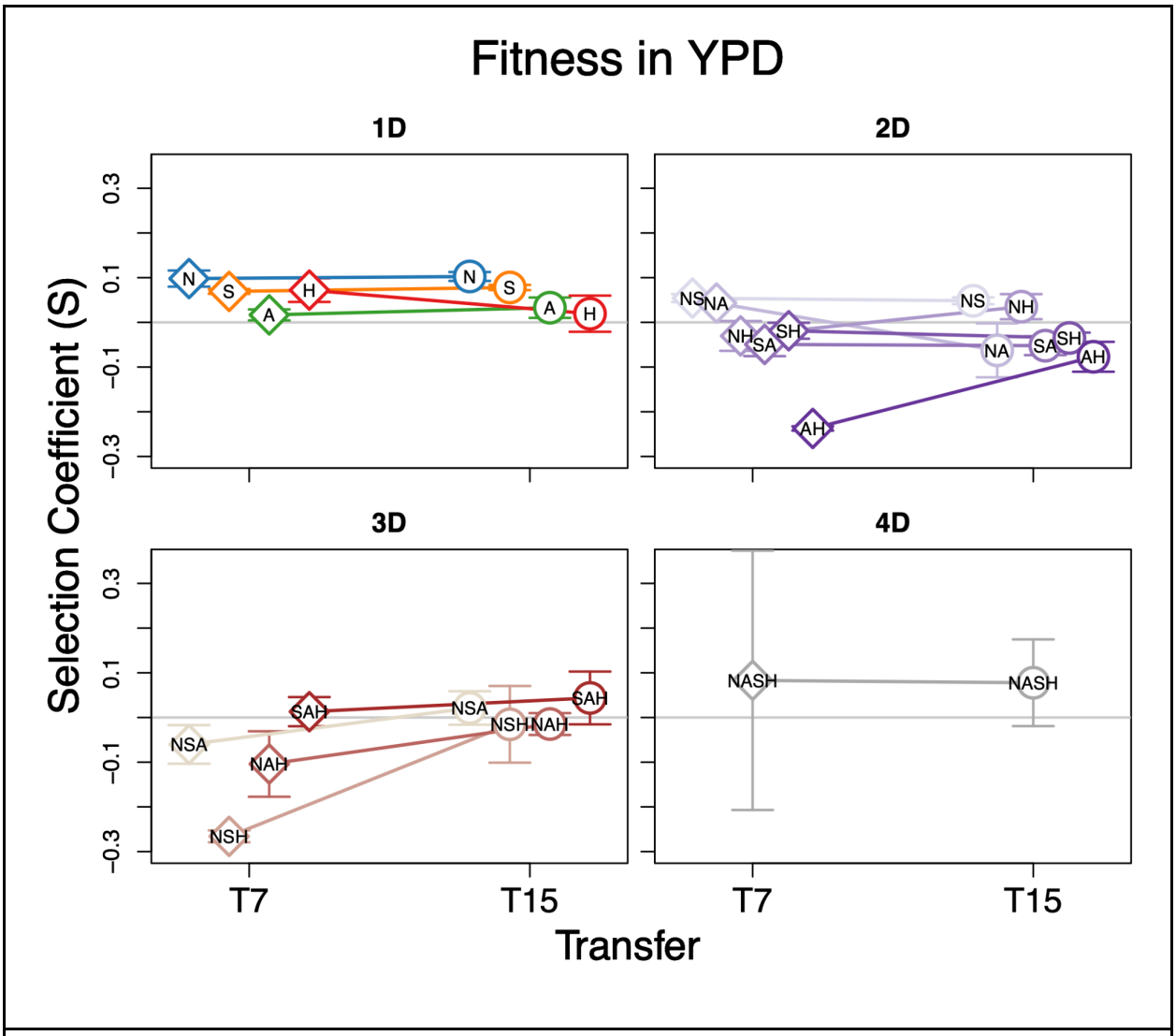

Fig 3. Cost of adaptation in the ancestral environment (YPD) for each evolved population partitioned by environmental complexity level (1D–4D). Estimated selection coefficients are shown as diamonds or circles for T7 and T15, respectively, with bars as standard deviations. The grey line represents a selection coefficient of 0. T0 is excluded for visualization purposes, as all points at T0 would fall on the zero-line.

Context 2: We then tested the fitness of each population in every environment it was not evolved in (e.g. N-evolved populations would be tested in S, A, and H individually, Fig 4). In non-selected environments, the strongest trade-offs across all evolved populations were initially observed in novel antifungal exposure (Fig 4; $\underline{S}_{A_T7}$=-0.210; Fig 4, upper right panel), and were subsequently reduced but rarely negated over the course of adaptation (

$\underline{S}_{A_T15}$=-0.133). Some positive pleiotropy was present as well, with the largest cross-adaptations occurring to novel NaCl exposure at T15 ($\underline{S}_{N_T15}$=0.032; Fig 4, upper left panel).

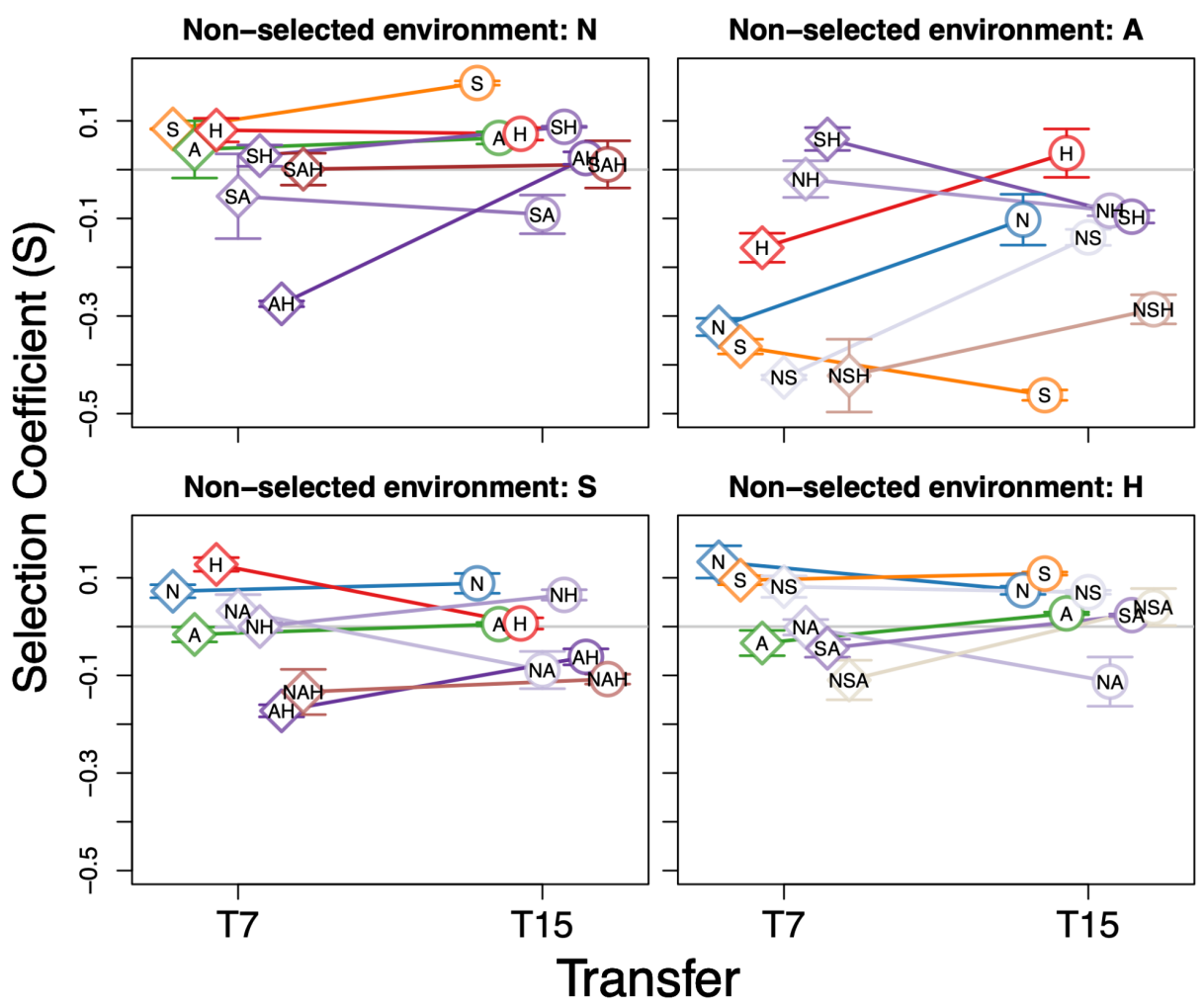

Fig 4. Trade-offs for evolved lines in their non-selected environments. Estimated selection coefficients are shown as diamonds or circles for T7 and T15, respectively, with bars as standard deviations. The grey line represents a selection coefficient of 0. T0 is excluded for visualization purposes, as all points at T0 would fall on the zero-line.

Context 3: Lastly we tested for trade-offs between adaptations to individual components of complex environments in ≥2D populations. All populations evolved in complex environments were unable to adapt to the same level as one or more 1D specialists in respective environmental components, resulting in apparent trade-offs (Fig

5). For each of the four single stressors, there were 7 complex environments that contained the individual stressor. The individual stressor with the fewest of the 7 complex environments reaching the same or greater fitness as the single-stressor population (i.e. with the largest proportion of trade-offs) was NaCl (1/7), followed by Starvation (4/7), Heat (4/7), and Antifungal (6/7) (Fig. S1). Despite the expectation and presence of prevalent trade-offs, some complex-adapted populations were able to exceed the fitness of the 1D specialist (Fig. S1; NS in Starvation, NAH and NSA in Antifungal, $p<0.05$).

As a measure of the degree to which ≥2D populations can adapt to individual stressors relative to 1D specialists, we took the ratio between the fitness of the ≥2D population tested in the single stressor (S_{nD_Ind}) and the maximum fitness of the associated single-stressor population at T15 (S_{1D_Ind}) as a "percentage of specialized fitness" ($\frac{S_{nD_Ind}}{S_{1D_Ind}}$). The trajectories of trade-off evolution for starvation and heat stress showed very strong initial trade-offs, which were later mitigated. At T7, populations exposed to starvation or heat had on average become maladapted to starvation and heat stress, reaching -5.1% (SD = 147.5%) and -190.3% (SD = 285.3%) of specialist adaptedness, respectively. The large magnitude in variation among treatments was primarily driven by the very strong trade-offs in NSH and SAH lines (Fig. S1). However, by T15, adaptation had increased to 52.9% (SD=74.3.1%) and 18.5% (SD=149.7%) for starvation and heat, respectively. Populations evolved in antifungal or salt showed more consistent positive adaptation over the course of the experiment, increasing from 57% (SD = 66.1%) to 88.5% (SD = 21.4%) and 18.1% (SD= 16.6%) to 46.9% (SD = 18.6%) on average, respectively (Fig. 5). These results suggest that, when present, adaptation typically occurs first to antifungal and that populations reach a higher "percent of specialized fitness" to antifungal than other stressors by T15. These adaptations may come at the cost of adaptedness to starvation and heat stress, though these maladaptations are typically compensated for by T15 (Fig. 5).

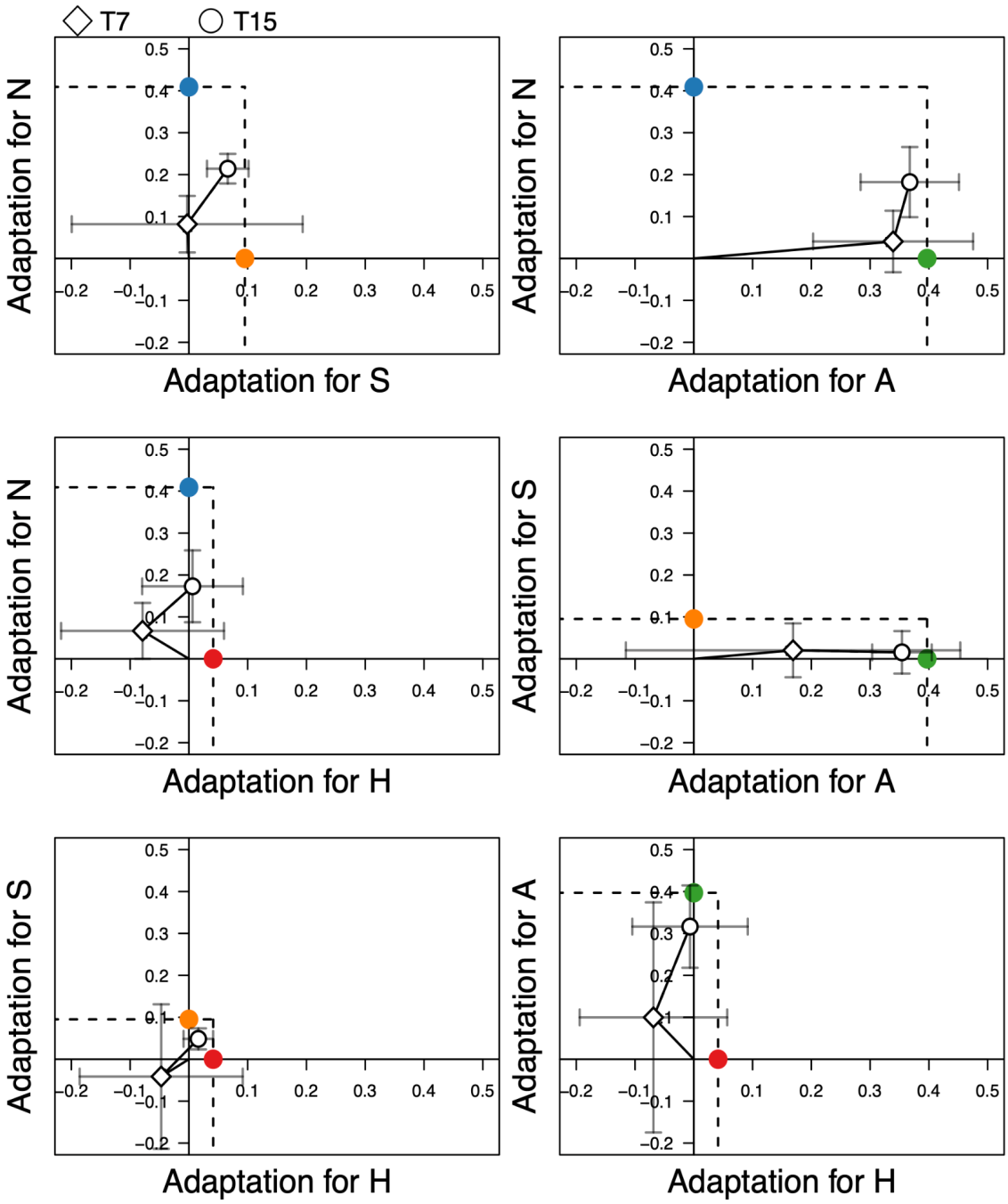

Fig 5. Trade-off trajectories of ≥2D populations visualized for every two-way combination of environmental components. For each panel, the means of all ≥2D populations evolved in those two environmental components are shown as diamonds or circles for T7 and T15, respectively. Standard deviations for selection coefficients are shown as bars for the respective axes (see Fig. S1 for individual treatments). Adaptation to the individual environment by the respective 1D population are shown as colored points projected along the respective axes. Within the lower-left of the black dotted lines represents the space in which complex environments are expected to fall (i.e. less adapted in single-environments than either 1D population).

Genomic dynamics

After filtering, we identified 228 SNPs and 57 INDELs across all timepoints and populations in our experiment. Populations varied moderately in SNP and INDEL number by T15 (mean = 3.91, SD=3.55), with some populations seemingly containing no SNPs (N3, N4, H3, NH1, NH2) while the highest number of variants was in A2 (n=18). Some of the populations with little to no mutations were N-evolved populations, which was unexpected considering that N-evolved populations show large and continued adaptation to the ancestor at each time point. One possibility for the lack of apparent mutations is that the ENA tandem array of genes (TAGs) in the strain S288c, which encode plasma membrane Na^+-ATPase exporters and are primary regulators during osmotic stress (Hohmann 2002), consist of three nearly identical sequences (Wieland et al. 1995). If putative mutations occurred in these TAGs, they would be filtered out by low unique mapping scores. We cover other possibilities in the discussion.

By T7, 21.6% (13/60) of populations had at least one mutation fix or nearly fix (AF>0.80), and the proportion of populations with fixed mutations increased to 31.6% (19/60) by T15 (Fig. 6). Multiple linear regression of the number of nearly fixed SNPs found per environment indicates some bias in the number of nearly fixed mutations at T15, where sweeps were more associated with evolving in antifungal (β=0.676, p<0.001) than salt and starvation (both β=0.363, p=0.037), and heat (β=0.176, p=0.305). Even for mutations at more moderate frequencies (AF>0.20), only 55% (33/60) of the populations contained at least one mutation at T7, and 66.6% (40/60) at T15.

Predicted effects of mutations by snpEff showed that across all populations, both SNPs and INDELs were primarily composed of mutations of at least moderate putative effect (Fig. S3). By T7, moderate-effect size mutations were the most predominant type of extant mutation across all populations (59/97), and 14 had nearly fixed in their respective populations. Relatively few high-effect mutations existed at T7 (10/129), but by T15 high-

effect mutations increased in appearance and frequency (56/179). All 9 low-effect mutations that existed at low frequencies (AF≤0.2) in T7 had been eliminated by T15.

We categorized mutations based on their putative gene ontology (GO) terms. We looked for mutations which were associated with osmotic stress (GO:0006970), response to starvation (GO:0042594), drug response (GO:2001023), or response to heat (GO:0009266). If the GO term of a mutation was found to be a lower-level GO term under one of these parent GO terms, it was grouped in the parent GO term category. Some mutations fell under multiple parent GO terms and were categorized separately. We found that populations typically contained mutations whose putative effects matched their evolved environment (Fig. 6). Most prominently though, every single population evolved in the presence of antifungal acquired mutations relating to drug responses with only five exceptions (A1, NAH1, SAH1, NASH1, and NASH4). All mutations for drug response fell within three genes (PDR1, PDR3, and PDR5), all of which encode for pleiotropic drug response (PDR) factors or transporters (Akache et al. 2004). Further, antifungal-related mutations are often the first to appear and rise in frequency in these populations before others. Some signs of clonal interference exist, where initially high frequency mutations (T7) fall, likely in response to the acquisition of a new mutation (e.g. A3, NA3, NASH4).

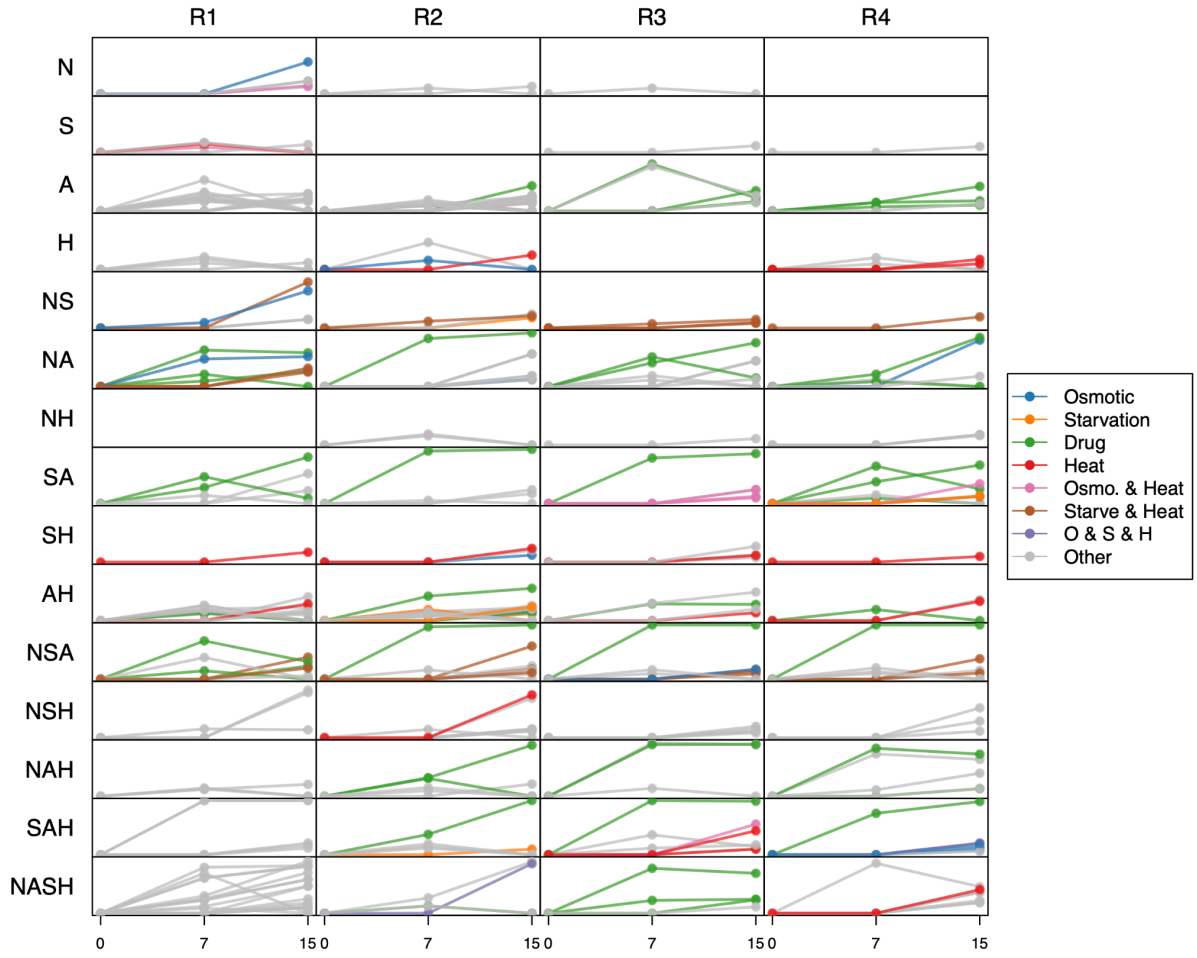

Fig 6. Allele frequency dynamics for each population. Points represent allele frequencies at time points at T0, T7, and T15. Points are colored by association with general gene-ontology terms: Response to osmotic stress, response to starvation, drug response, and response to heat. Some mutations have overlapping GO terms, and are colored separately for each type of overlap. Replicates are designated as R1–R4.

We then searched for potential copy number variants at both the whole-chromosome and sub-chromosome level. At the chromosome level, we observed that chromosome 12 showed consistent patterns of copy number gain across several replicates (NSA1, NSA3, NAH1, SAH1, NASH1) while one instance of chromosome 14 was elevated (also in NAH1) (Supp. Fig. 3). Although performing an enrichment analysis may not produce meaningful outcomes across an entire chromosome, we can speculate on possible relevant genes which exist on Chromosome 12 and 14. Chromosome 12 contains genes related to known pleiotropic drug resistance (PDR8, TOP1, CIS1), osmotic stress (FPS1,

RCK2, STE11, SGD1, SSK1), glucose limitation (SSA2, YPT2, GSY2,ECM30, FBP1), and heat stress (SSQ1, SYM1, GSY2, HSP60,HSP104, SSA2). Chromosome 14 contains genes for osmotic stress (VAC7, POR1, SSK2, INP52,SKO1, FIG4), pleiotropic drug response (MKT1,HCH1, PDR16,HDA1), and heat stress (HCH1, WSC2,HDA1,YDJ1, NMA111).

Within individual chromosomes, only two partial CNVs were identified in all populations (Supp. Fig 4). The first in NAH1 between 90kb–150kb on Chromosome 3 (spanning 35 genes) at both T7 and T15, and the second in SAH2 only at T7 between 46kb–70kb on chromosome 15 (spanning 14 genes). The partial CNV in NAH1 contains genes related to salt homeostasis (SAT4,RVS161), and the CNV in SAH2 contains genes related to glycolysis (PFK27) and transcriptional response to glucose starvation (RTC1).

Gain or loss of putative compensatory mutations during trade-off evolution

We found several fitness trade-offs for simultaneously-selected stressors in all populations at T7, many of which were maladapted to one of the individual components of their complex environment. However, most trade-offs resulting in negative fitness at T7 had been mitigated by T15 such that relative fitness had at least increased to nearly neutral (≈0) or positive values (Fig S1). If mitigation of trade-offs resulting in maladaptation was due to compensatory gain or loss of *de novo* mutations, we may pair increases in fitness with the gain or loss mutations between T7 and T15 in an attempt to uncover putative compensatory mutations. Here we consider compensations found in ≥2D populations which show large negative fitness in an individual stressor at T7 that become mitigated or reversed by T15, and focus on examples of populations exhibiting the largest compensations. For each example, we only discuss mutations that reached an appreciable frequency (AF>0.10) at either time point; higher frequency mutations more likely contributed to mean population fitness during the time of sampling and phenotyping. For each loss or gain of a mutation, we briefly describe its primary known association in parentheses according to the *Saccharomyces* Genome Database (Cherry et al. 1998).

The populations which showed the largest compensations in the resistance of antifungal are NSA1 (S_{T7} = -0.161, S_{T15}= 0.492), SAH3 (S_{T7} = -0.402, S_{T15}= 0.371), and SAH4 (S_{T7} = -0.345, S_{T15}= 0.488). In NSA1, compensations between T7 and T15 were notably

associated with the loss of one PDR1 mutation and the gain of another PDR1 mutation at a different position, as well as the loss of two RIM15 mutations (associated with cell proliferation). SAH3 gained two mutations in PUF3 (mRNA regulation of mitochondrial biogenesis), and one in PSR1 (general stress response). SAH4 also gained a mutation in PSR1, as well as SOD1 (general stress response) and ROX1(regulator of ergosterol levels). Notably for ROX1, the mechanism of action for fluconazole includes inhibition of ergosterol synthesis, disrupting cell wall permeability (Spampinato et al., 2013).

In populations evolving to the presence of salt, NSA3 (S_{T7} = -0.052, S_{T15}= 0.200) , NSA4 (S_{T7} = -0.026, S_{T15}= 0.223), and NASH1 (S_{T7} = -0.224, S_{T15}= 0.102) showed the largest compensations. Both NSA3 and NSA4 gained mutations at different positions in the gene RIM15 (associated with cell proliferation). NSA3 additionally gained a mutation in MYO5 (motor protein associated with cytoskeletal integrity), while NSA4 gained a mutation in GPI17 (cell wall integrity) and lost a mutation in TEC1 (transcription factor of filamentation genes). NASH1 gained mutations in SKY1 (cation uptake and homeostasis) and PRC1 (vacuolar exopeptidase), and lost a mutation in CSG2 (calcium homeostasis).

All NSH populations showed initially strong trade-offs for both starvation (S = -0.24 – -0.309) and heat (S = -0.2 – -0.286). However, by T15, these trade-offs were mitigated or reversed for starvation (S = -0.019 – 0.194) and heat (S = -0.07 – 0.09). NSH1 gained mutations in SAC3 (bud morphology) and MCM1 (G2/M transition of mitosis). NSH2 acquired mutations in IRA2 (general stress response), PUF3, OKP1 (kinetochore assembly), and THP2 (transcription elongation), while losing a mutation in AUR1 (sphingolipid synthesis). NSH3 acquired new mutations in SUB2 (mRNA splicing and export), SAC3 (mRNA export and transcriptional elongation), and EEB1 (medium-chain fatty acid biosynthesis). NSH4 gained mutations in SUB2, SNF7 (sorting of transmembrane proteins), and RTG1 (mitochondria-nucleus signal transduction).

While some genes identified with gains or losses of mutations are associated with their respective compensatory adaptations, and others are associated with general stress responses (IRA2, PSR1, SOD1), few of the gene mutations have obvious known phenotypic effects for the environments the mutations were observed in. Although it could be the case

that the identified genes do not play a role in compensatory adaptations during the evolution of trade-offs, we here focused on genic mutations which reached an allele frequency of at least 10%, indicative of some adaptive role for observed mutations. Assuming that these mutations do play a role in trade-off evolution, it is clear that many have pleiotropic effects which have yet to be described in detail. Further, putative compensations between T7 and T15 were primarily driven by the acquisition of new mutations rather than the loss of segregating mutations in the populations.

Phenotypic and genomic parallelism

Using a linear model to test for significant variation in fitness as a function of complexity, we find that on average across all samples, variation among replicates increased with environmental complexity at T7 , but not at T15 (Fig. 7). Thus, adaptation was less phenotypically parallel in more complex environments, but only early in adaptation. There is not a clear pattern of replicates continuing to diverge over the course of adaptation as complexity increases. Because increased environmental complexity is associated with increased stressor effects, we ran additional regressions including stressor effect as the sole effect and as a covariate with complexity. Stressor effects did not significantly explain variation at either time point in any model or model comparison ($p>0.05$).

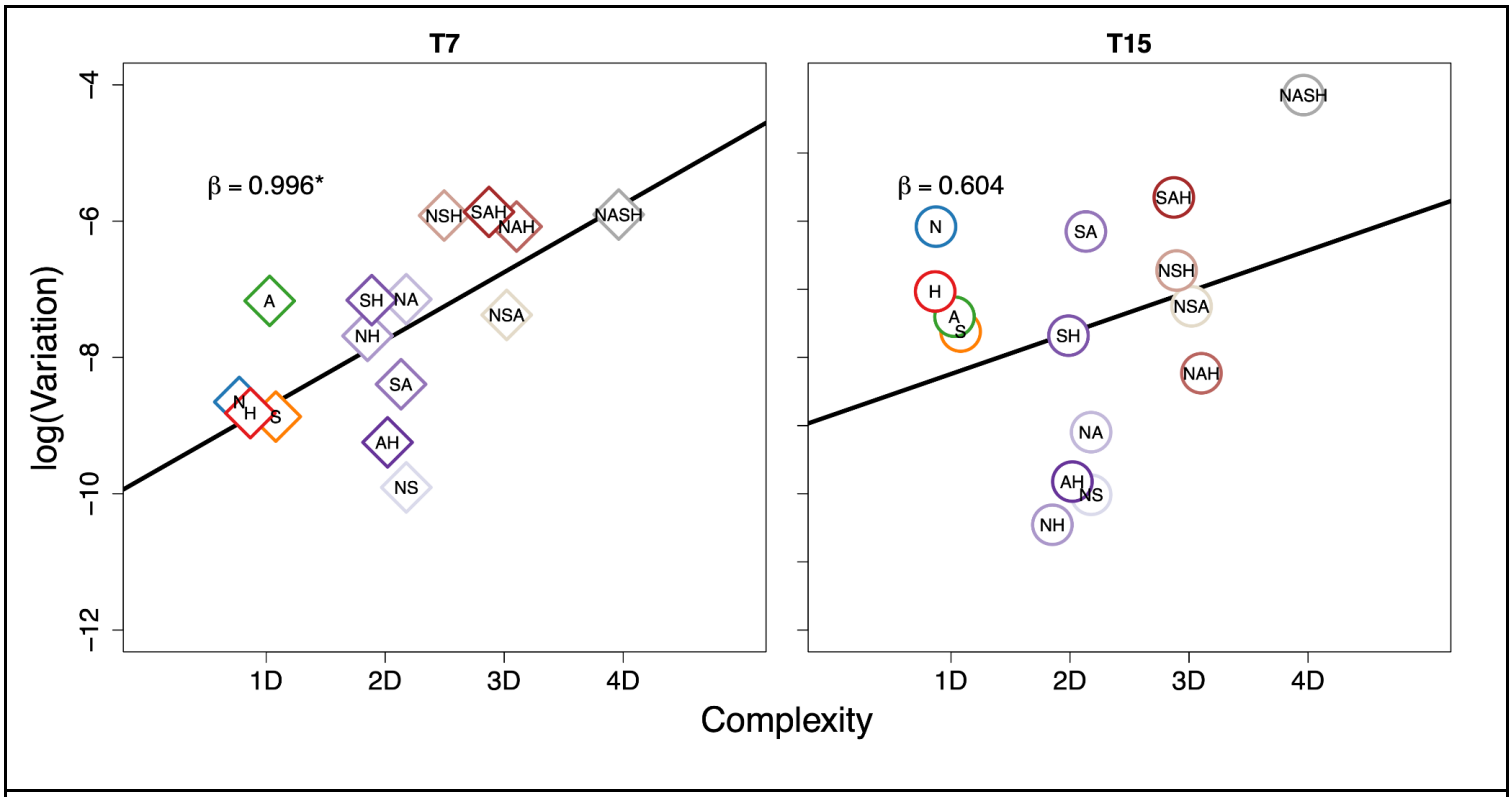

Figure 7: Linear regressions of environmental complexity on log variation of selection coefficients. Points are jittered along the x-axis. The regression is plotted as the black line. A significant slope is denoted with an asterisk. See Fig S5 for comparisons of variation change for each environment.

Observed parallelism was high at the gene level (Fig. 8), with shared gene mutations appearing in up to 18 independent populations. The PDR family of genes again shows increased prevalence in shared gene mutations across most populations evolved in the presence of antifungal. PDR1 in particular shows the highest number of shared gene mutations with 18 shared mutations. The second-highest number of shared gene mutations occurred in PUF3, present in many populations evolving to high heat. The prevalence of PUF3, associated with heat tolerance, is surprising considering that H and SH populations often showed little to no change in fitness from the ancestor (Fig 2), and high heat imposes the lowest stressor effect (Fig 1C). Many shared genes do not have an apparent connection to adaptation to any of the four main stressors, and are not related to general stress responses (except SUB2 and IRA1).

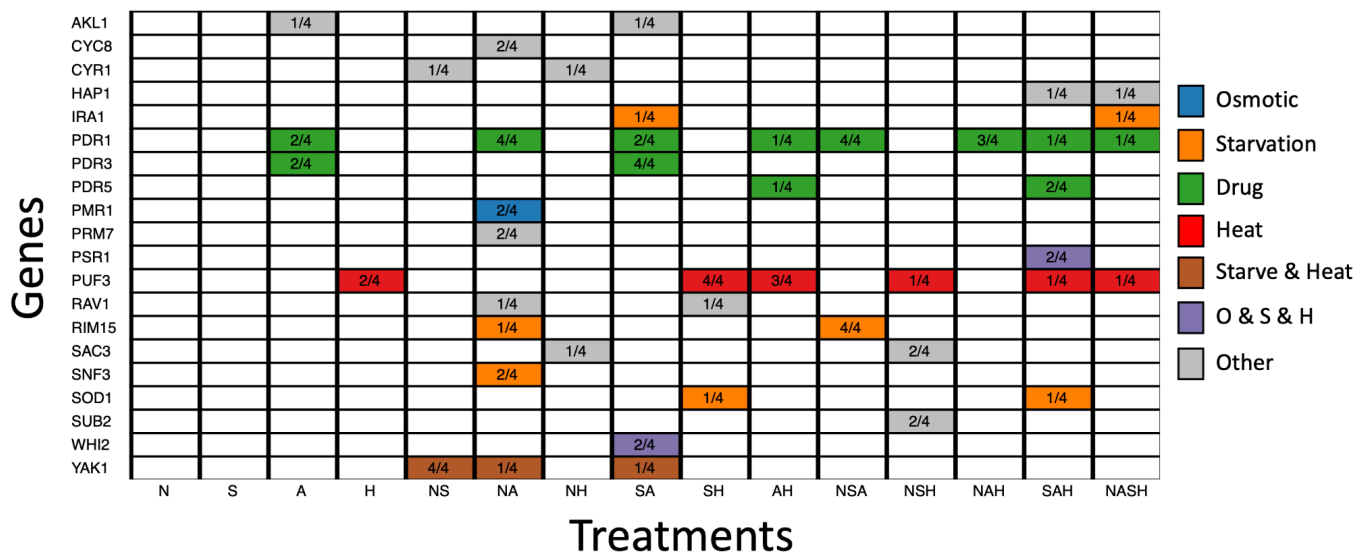

Figure 9. Recurrent mutations across independent evolved populations. Shared mutations are colored by the parental GO category, white indicates no shared mutation.

At the nucleotide level, we found evidence of parallelism in the form of recurrent *de novo* mutations (Fig. 9). In total, 10 *de novo* populations were shared between two, or even three, populations at the end of the experiment in T15. The most striking recurrent mutations are for the genes PDR1 and PUF3. In PDR1, one of the genes which encodes for pleiotropic drug response factors, two recurrent mutations were observed; two recurrent mutations in one position, and two recurrent mutations in a second position, all in populations evolved in the presence of the antifungal. PUF3, associated with the regulation of mRNA degradation, appears repeatedly in 3 populations in one position, and in 2 populations in the other position. Although not associated with the GO term for heat resistance, PUF3 has been shown to be associated with resistance to heat shock in empirical experiments (Harris et al. 2005; Jarolim et al. 2013).

A mutation in SAC3, which has been shown to cause bud (Watanabe et al. 2009) and cell size (Watanabe et al. 2009; Jorgensen et al. 2002) morphological changes, as well as increased heat resistance in S288c (Jani et al. 2009), was seen in NSH1 and NSH3. YAK1, observed in NS1 and NS3, encodes for a regulator of a glucose-deprivation stress response system (Moriya et al. 2001). SH2 and SAH4 share SOD1, a gene in which mutations have

been shown to double the lifespan of yeast during stationary phase (Harris et al. 2005). S3 and S4 share a mutation upstream of MLF3, which has unknown function, but whose overexpression has been shown to decrease vegetative growth rates (Sopko et al. 2006). Upstream mutations for DFP1 and YDL228C were also observed, though are of unknown or dubious functionality, respectively.

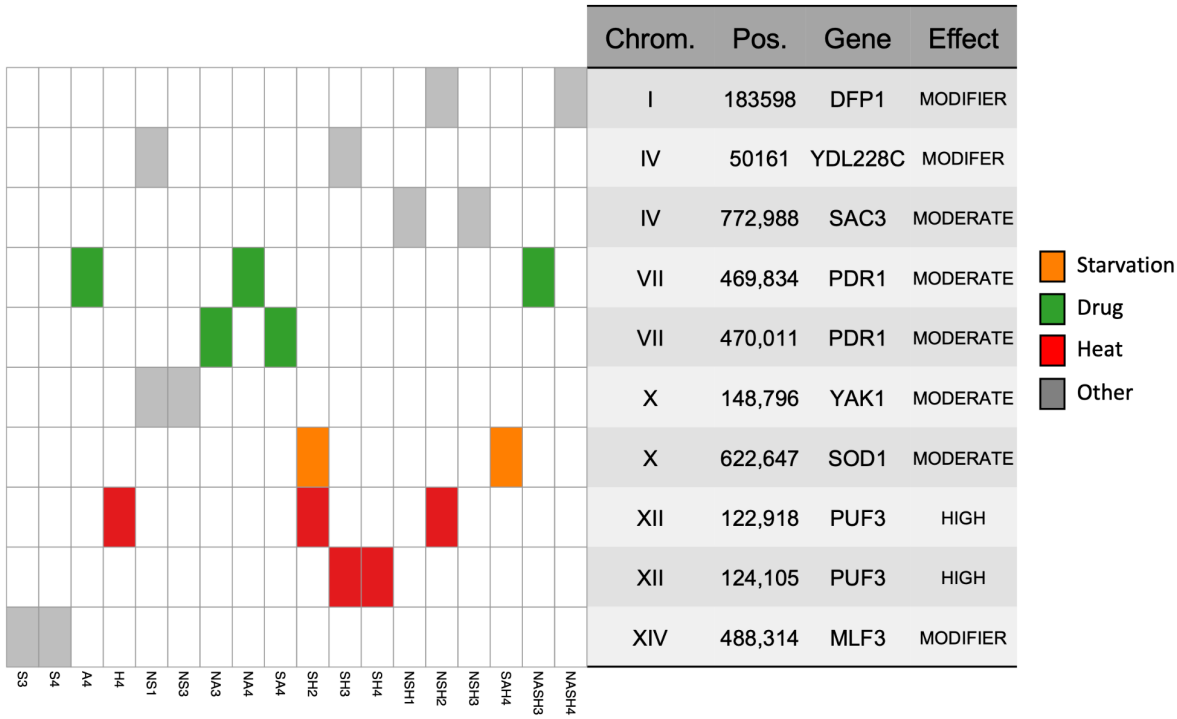

Chrom.	Pos.	Gene	Effect
I	183598	DFP1	MODIFIER
IV	50161	YDL228C	MODIFER
IV	772,988	SAC3	MODERATE
VII	469,834	PDR1	MODERATE
VII	470,011	PDR1	MODERATE
X	148,796	YAK1	MODERATE
X	622,647	SOD1	MODERATE
XII	122,918	PUF3	HIGH
XII	124,105	PUF3	HIGH
XIV	488,314	MLF3	MODIFIER

Figure 9. Recurrent mutations across independent evolved populations. Shared mutations are colored by the parental GO category, light grey is no shared mutation. The table presents the chromosome, position, gene name, and predicted effect given by SnpEff for each mutation. Populations which do not contain a recurrent mutation are not shown.

Discussion

Adaptation Dynamics

We observed rapid fitness increases over the course of 15 serial transfers in most treatments and populations (Fig. 2). At lower complexity levels (≤2D), it appeared that fitness had at least temporarily plateaued between the mid- and end-point of the

experiment. Previous experiments of microbial evolution from *de novo* mutations showed similar increases in fitness followed by a plateau (Wiser et al., 2013; Johnson et al., 2021). However, we also observed that populations in higher environmental complexities continued to adapt between T7 and T15 to a moderate degree. These patterns of diminishing fitness gains are consistent with both the Fisher Geometric Model (FGM) of adaptation (Tenaillon, 2014) and the diminishing returns epistasis (DRE) model of adaptation (Wei & Zhang, 2019). Whereas the FGM predicts that mutations of large effect are less likely to contribute to adaptation as populations increase in fitness due to potentially overshooting a fitness optimum, the DRE model predicts that any given beneficial mutation will demonstrate smaller effects when present on an already fit genetic background. These models are not mutually exclusive, and both may be useful in understanding empirical dynamics of adaptation. Given that higher environmental complexities result in higher stressor effects, and thus populations initially residing further away from a fitness optimum, our patterns of diminishing rates of adaptation align well with these theoretical expectations. Fisher also predicted that adaptation to an increasing number of traits should rely on mutations of small effect (Fisher, 1999). Later, Kimura (1979) and Orr (1998) showed that mutations of small effect are easily lost. As a consequence of these theoretical predictions, it is expected that mutations of intermediate effect size are the most likely to contribute towards adaptation. Indeed, we see evidence that a majority of mutations are estimated to have moderate effect sizes (Fig. S2), further supporting a FGM view of adaptation in our system.

There were some surprising exceptions to adaptation over the course of the experiment; H and SH populations increased very little in fitness relative to the ancestor by T15 (Fig. 2). The lack of apparent adaptation in H and SH populations is perhaps due to the relatively low stressor effects of heat and starvation (Fig. 1B). In another experimental evolution study in *S. cerevisiae*, populations evolved in environments with low stressor effects also showed little to no increases in fitness over the course of 1,000 generations (Ament-Velasquez et al., 2022). However, the frequent recurrent mutations observed in heat-adapting populations for the gene PUF3 are suggestive of adaptive evolution (Fig. 8). Other studies have shown that populations with higher initial fitness, such as those evolved

with low stressor effects, adapt more slowly (Kryazhimskiy et al., 2014). Given more time to evolve, H and SH populations may demonstrate clearer signs of adaptation.

At the genomic level, we observed the appearance and subsequent rise in frequency of SNPs, INDELs, and copy number variants during evolution (Fig 6, S4). In our experiment, genomic evolution is sometimes characterized by rapid sweeps, most prominently in mutations related to pleiotropic drug responses in populations evolving with the antifungal. However, a majority of populations do not contain mutations that sweep to fixation, and some even show an apparent lack of any mutations (Fig 6). This is most striking in salt-adapted populations, which show consistent increases in adaptation relative to the ancestor (Fig 2). We suspect that we may be missing mutations due to conservative filtering steps. In particular, there are three paralogous genes which encode for sodium pumps (ENA1, ENA2, ENA5) which arose from tandem duplications. The sequences of these tandem array duplications are nearly identical, causing reads to map to each copy of ENA and receive low mapping scores which are subsequently filtered out. If putative mutations arose in these key sodium-regulating genes, they would be filtered out during our analysis. However, we do see mutations in other osmotic-regulation genes (Fig. 6) in other populations adapting to salt-containing environments.

An alternative explanation for the apparent lack of mutations and sweeps seen in the genomes is that many of the changes in fitness we observed are due to epigenetic changes. The degree of osmotic stress, nutrient stress, and heat stress are all likely to be variable in natural populations of yeast, and phenotypic plasticity may already exist for resistance to these stressors. For example, a study in *S. cerevisiae* and *Schizosaccharomyces pombe* showed that descendants of yeast exposed to sub-lethal doses of salt had an increased resistance to higher doses of salt relative to non-exposed ancestors (Gonzalez and Bell 2013). Although this study was not able to quantify the degree to which resilience was due to genetic or epigenetic changes, it remains a possibility. Trans-generational epigenetic changes may also slow or prevent evolution by reducing the efficacy of selection on new mutations (Fox et al. 2019). We intend to implement further experiments to test for the effect of epigenetic changes in our evolved yeast populations to account for this.

Several mutations identified with a relevant parent GO term were seen in associated environments (Fig 6). However, many other instances exist in which mutations with no apparent relevant GO term increased in frequency during the experiment. Although not many of these unassociated mutations increased to appreciable levels (AF>0.10) by T15, it is possible that many of these mutations have either general stress responses or undescribed pleiotropic effects (see below for further discussion of pleiotropy).

Evolution of trade-offs

Trade-offs were abundant and clearly observed across three distinct contexts: (1) the ancestral environment (Fig 3), (2) non-selected environments (Fig 4), and (3) simultaneously selected stressors (Fig 5). The dynamics of these trade-offs underwent shifts throughout the process of adaptation. Trade-offs across all the ancestral environments were initially very strong at T7, but then often negated or even reversed by T15. Considering that the ancestral medium (YPD) was the basis for all other stressors (exception for the starvation treatment, where glucose was decreased), these fitness costs could be interpreted as the cost of stressor removal in adapted populations. However, the removal of stressors from evolved populations did not always increase fitness, as seen in evolved rotifers exposed to their ancestral environment without stressors (Orr et al. 2022).

Trade-offs in non-selected (novel) environments were surprisingly less prevalent and showed different patterns across environments. Many populations showed trade-offs when exposed to antifungal, but the effects of these trade-offs were reduced in populations sampled at T15. It is unclear what physiological or molecular changes might cause such strong effects in populations exposed to antifungal. Fluconazole functions by inhibiting the fungal cytochrome P450 enzyme 14-demethylase, which has the downstream effect of decreasing cellular permeability (Spampinato and Leonardi 2013). Because stress responses to osmotic stress, low glucose, and heat shock often involve changes in cellular permeability (Bermejo et al. 2010; Piper 1995; Hohmann 2002), effects of fluconazole may have strong interactive effects with adaptive changes to other stressors. Contrary to the negative pleiotropic effects found with fluconazole, the other three non-selected environments showed largely positive pleiotropy, perhaps for similar reasons.

Fitness assays showed that no population evolving in a complex environment was able to reach the level of fitness in all respective individual environments as the populations evolved solely in those single stressors. But being unable to optimally adapt to all exposed stressors did not preclude populations from adapting to multiple stressors simultaneously. Adaptation to antifungal typically showed the highest initial rates of adaptation, increasing on average to 57% of the antifungal specialist's final fitness by T7, and reaching 88.5% by T15. Despite the presence of salt imposing the strongest individual selection pressure, the rate of adaptation and "percent of specialized adaptation" to salt was only secondary to antifungal. When in the presence of starvation or heat, salt adaptation typically occurred first and reached a greater "percent of specialized adaptation". This indicates that the ease of mutational access to antifungal resistance drives early adaptation and trade-off dynamics, but the strength of selection determines adaptive dynamics among treatments in which the basis of adaptation may be more polygenic. The ease of mutational accessibility for antifungal resistance is apparent in the proportion of populations which reached or exceeded the specialist level of fitness (6/7). On the contrary, only 1/7 respective complex-evolved populations reached a fitness equal to that of the salt specialist.

Despite not reaching the same fitness as 1D populations in respective environments, some ≥2D populations surprisingly showed fitness surpassing that of 1D populations in at least one of the respective individual environments (Fig S1), indicating that some mutations had strongly positive pleiotropic effects in complex environments. Positive pleiotropy has been observed in a study of DNA bacteriophages evolving in complex environments (McGee et al. 2016) with selection on both growth rate and capsid stability. Despite expectations of antagonistic pleiotropy between these traits, when selection for capsid stability was increased, mutations increasing capsid stability also positively affected growth rate, suggesting that stronger selection in complex environments forced populations to exploit mutations that enhanced multiple traits under the threat of extinction, thus overriding the trade-off costs associated with a complex selective environment.

We observed significant negative trade-offs in several other complex-stressor populations at T7, particularly for environments including heat and starvation (Fig S1). However, by T15, these negative trade-offs were frequently nullified or even reversed. We found that many gene mutations without clear functions related to the relevant environment appeared and rose in frequency during these trade-off dynamics. The lack of gene mutations with known associations to the respective environments is indicative of compensatory mutations often having pleiotropic effects across several traits, or perhaps indirectly affecting fitness in those environments through interactions with relevant gene networks (Szklarczyk et al. 2023). Although we focused primarily on gene mutations associated with trade-offs in selected individual environments, we also saw stark shifts in trade-off magnitude and direction in both the ancestral YPD environment and non-selected environments, which may be caused by mutations of pleiotropic effect (Szamecz et al. 2014). Future work could functionally validate the pleiotropic effects of observed mutations through cloning of single or multiple mutations in an ancestral background to isolate mutational and epistatic effects.

Parallelism at the genomic and phenotypic level

Because mutations show many-to-one mapping towards fitness (Barghi, Hermisson, and Schlötterer 2020), we expect increasing parallelism at higher organizations of biological scale, from base pair mutations culminating to fitness. Despite this, theory does predict that recurrent *de novo* mutations are likely in populations with either large population size or high mutation rate (Pennings and Hermisson 2006). Adaptive recurrent *de novo* mutations have been observed in a range of systems, from viruses (Bedhomme, Lafforgue, and Elena 2013) to *Aribadopsis* (Konečná et al. 2021), and humans (Hamblin and Di Rienzo 2000). Not only is the mutation rate in *S. cerevisiae* on par or higher than that of many other eukaryotes (Baer, Miyamoto, and Denver 2007; Lynch et al. 2008), but our experimental setup allowed for very large effective population sizes ($\sim 1\times10^7$ cells in a saturated 5ml tube). By the end of experimental evolution, we had observed 10 recurrent *de novo* mutations between independent populations. Of these, 3 recurrent mutations were observed in a gene responsible for pleiotropic drug responses (PDR1). Drug resistance evolution is often highly parallel at the mutational level, such as in HIV drug resistance

(Pennings, Kryazhimskiy, and Wakeley 2014), multidrug resistance in Malaria (Nair et al. 2007), fungicide resistance (to a lesser extent herbicide and insecticide resistance; (Hawkins et al. 2019), and resistance to chemotherapy drugs in *S. cerevisiae* (Vázquez-García et al. 2017).

Although we cannot completely rule out the possibility of cross-contamination, particularly for populations whose experimental evolution was conducted concurrently (S3/S4, NS1/NS3, SH3/SH4,NSH1/NSH3), each population only shares up to one recurrent mutation with any other population. That populations do not share sets of mutations indicates that the appearance of these mutations is the result of independent mutational events. Additionally, serial transfers for populations in different environments were conducted at different times, sometimes weeks apart, reducing the likelihood of cross-contamination. The additional use of independent glass tubes for each population further reduces the risk of cross-contamination relative to the use of 96-well plates common in yeast experimental evolution.

Repeated mutations at the gene level were expected, and are common in other experiments with *S. cerevisiae* (Johnson et al. 2021; Ament-Velásquez et al. 2022). Johnson et al. (2021) focused on populations experiencing relatively benign environments (YPD & SC at 30C, though also included a high heat treatment at 37°C in SC), and found many multi-hit genes which were not specific to treatment. In contrast, we found that genes of a particular gene-ontology were typically associated only with evolution in an associated environment. For example, we saw a high representation of the PDR network of genes only in environments evolved with antifungal. Likewise, PUF3 mutations, associated with heat stress, were found only in populations adapting to high heat.

There are several complementary explanations for our observed patterns of parallelism at the mutational and genic level. We saw that populations exposed to fluconazole had an enrichment of mutations at both the base pair and gene level. Fluconazole has known genotoxic effects, increasing the rate of DNA damage (Silva et al. 2019; Yüzbaşioğlu et al. 2008; Ribeiro et al. 2022). Increased parallelism at the genomic level may be due to increased mutational availability in antifungal-exposed populations.

This may be compounded by antifungal resistance having a simple genetic basis; many drug resistances occur due to the loss- or reduction-of-function mutations in a single gene inhibiting the uptake or molecular binding of drugs (Bavro, Conn, and Davies 2019). It is also known that mutation rates can vary widely across the genome (Lang and Murray 2008), and genes in which recurrent mutations appear may be located in mutational hotspots. Another common recurrent mutation we observed in the gene PUF3 is associated with strong compensations for fitness in high heat during trade-off evolution in many hot-adapting populations. It could be that despite having a low individual stressor effect, heat produces strong synergistic stressor effects, necessitating the recurrent evolution of mutations associated with heat stress.

The selection coefficients we measured represent relative fitness only in that tested environment, which precludes us from testing parallelism in fitness between environments. However we observed relatively high parallelism in fitness within replicates of each environment, with the exception of the most complex environment, NASH. We asked whether the degree of complexity affects the variation in fitness observed and found that variation between replicates does increase with the level of complexity, but primarily in the first half of our experiment (T0 to T7). This indicates that populations evolving in environments with lower complexity begin diverging in fitness later in adaptation. This pattern is not explained by either the initial stressor effects of each environment, nor associated with any of the four stressors. This suggests that, in simple environments, mutations that emerge first in populations tend to have a more homogenous effect on fitness.

Conclusions

Our study shows that the dynamics of adaptations and trade-off evolution in complex environments are affected by the degree of environmental complexity, and the physiological and genetic interactions between environmental components. The strength of selection of individual components determined early adaptive dynamics in our evolution experiment, but the genetic basis and ease of mutational accessibility determine the order and degree of trade-off evolution. Recurrent gene mutations in complex environments

associated with single stressors of low stress effect are also indicative of the influence potential synergistic interactions have on adaptive dynamics. Understanding the outcomes of evolution to complex environments is of interest to both evolutionary biologists and conservationists. Our results highlight that we need a deeper mechanistic understanding of contemporary stressor effects on organisms and the genetic basis of resistance in order to not only explain, but predict evolutionary outcomes in populations evolving in ecologically relevant environments.

Acknowledgements

Thanks to Carla Bautista, Mario Walthert, Sofia Rouot, and Ciaran Gilchrist who assisted in growth-curve and flow cytometry measurements. The computations and data handling were enabled by resources in project [NAISS 2023/23-487] provided by the National Academic Infrastructure for Supercomputing in Sweden (NAISS) at UPPMAX. This work was supported by the Swedish Research Council (2017-04963 and 2022-03427 to RS) and the Knut and Alice Wallenberg Foundation (2017.0163 to RS).

References

Abbey, Darren A., Jason Funt, Mor N. Lurie-Weinberger, Dawn A. Thompson, Aviv Regev, Chad L. Myers, and Judith Berman. 2014. "YMAP: A Pipeline for Visualization of Copy Number Variation and Loss of Heterozygosity in Eukaryotic Pathogens." *Genome Medicine* 6 (11): 100.

Agrawal, Anurag A. 2017. "Toward a Predictive Framework for Convergent Evolution: Integrating Natural History, Genetic Mechanisms, and Consequences for the Diversity of Life." *The American Naturalist* 190 (S1): S1–12.

Akache, Bassel, Sarah MacPherson, Marc-André Sylvain, and Bernard Turcotte. 2004. "Complex Interplay among Regulators of Drug Resistance Genes in Saccharomyces Cerevisiae." *The Journal of Biological Chemistry* 279 (27): 27855–60.

Ament-Velásquez, Sandra Lorena, Ciaran Gilchrist, Alexandre Rêgo, Devin P. Bendixsen, Claire Brice, Julie Michelle Grosse-Sommer, Nima Rafati, and Rike Stelkens. 2022. "The Dynamics of Adaptation to Stress from Standing Genetic Variation and de Novo Mutations." *Molecular Biology and Evolution* 39 (11). https://doi.org/10.1093/molbev/msac242.

Baer, Charles F., Michael M. Miyamoto, and Dee R. Denver. 2007. "Mutation Rate Variation in Multicellular Eukaryotes: Causes and Consequences." *Nature Reviews. Genetics* 8 (8): 619–31.

Barghi, Neda, Joachim Hermisson, and Christian Schlötterer. 2020. "Polygenic Adaptation: A Unifying Framework to Understand Positive Selection." *Nature Reviews. Genetics* 21 (12): 769–81.

Barrett, Rowan D. H., R. Craig MacLean, and Graham Bell. 2005. "Experimental Evolution of Pseudomonas Fluorescens in Simple and Complex Environments." *The American Naturalist* 166 (4): 470–80.

Bavro, Vassiliy, Graeme L. Conn, and Christopher Davies. 2019. *Bacterial Mechanisms of Antibiotic Resistance: A Structural Perspective*. Frontiers Media SA.

Bedhomme, Stéphanie, Guillaume Lafforgue, and Santiago F. Elena. 2013. "Genotypic but Not Phenotypic Historical Contingency Revealed by Viral Experimental Evolution." *BMC Evolutionary Biology* 13 (February): 46.

Bennett, Albert F., and Richard E. Lenski. 2007. "An Experimental Test of Evolutionary Trade-Offs during Temperature Adaptation." *Proceedings of the National Academy of Sciences of the United States of America* 104 Suppl 1 (Suppl 1): 8649–54.

Bermejo, Clara, Farzad Haerizadeh, Hitomi Takanaga, Diane Chermak, and Wolf B. Frommer. 2010. "Dynamic Analysis of Cytosolic Glucose and ATP Levels in Yeast Using Optical Sensors." *Biochemical Journal* 432 (2): 399–406.

Bono, Lisa M., Leno B. Smith Jr, David W. Pfennig, and Christina L. Burch. 2017. "The Emergence of Performance Trade-Offs during Local Adaptation: Insights from Experimental Evolution." *Molecular Ecology* 26 (7): 1720–33.

Bonsall, Michael B., and Marc Mangel. 2004. "Life-History Trade-Offs and Ecological Dynamics in the Evolution of Longevity." *Proceedings. Biological Sciences / The Royal Society* 271 (1544): 1143–50.

Cherry, J. M., C. Adler, C. Ball, S. A. Chervitz, S. S. Dwight, E. T. Hester, Y. Jia, et al. 1998. "SGD: Saccharomyces Genome Database." *Nucleic Acids Research* 26 (1): 73–79.

Cingolani, Pablo, Adrian Platts, Le Lily Wang, Melissa Coon, Tung Nguyen, Luan Wang, Susan J. Land, Xiangyi Lu, and Douglas M. Ruden. 2012. "A Program for Annotating and Predicting the Effects of Single Nucleotide Polymorphisms, SnpEff: SNPs in the Genome of Drosophila Melanogaster Strain w1118; Iso-2; Iso-3." *Fly* 6 (2): 80–92.

Cisneros-Mayoral, Sandra, Lucía Graña-Miraglia, Deyanira Pérez-Morales, Rafael Peña-Miller, and Ayari Fuentes-Hernández. 2022. "Evolutionary History and Strength of Selection Determine the Rate of Antibiotic Resistance Adaptation." *Molecular Biology and Evolution* 39 (9). https://doi.org/10.1093/molbev/msac185.

Danecek, Petr, James K. Bonfield, Jennifer Liddle, John Marshall, Valeriu Ohan, Martin O. Pollard, Andrew Whitwham, et al. 2021. "Twelve Years of SAMtools and BCFtools." *GigaScience* 10 (2). https://doi.org/10.1093/gigascience/giab008.

Elena, Santiago F., and Richard E. Lenski. 2003. "Evolution Experiments with Microorganisms: The Dynamics and Genetic Bases of Adaptation." *Nature Reviews. Genetics* 4 (6): 457–69.

Elmer, Kathryn R., Shaohua Fan, Henrik Kusche, Maria Luise Spreitzer, Andreas F. Kautt, Paolo Franchini, and Axel Meyer. 2014. "Parallel Evolution of Nicaraguan Crater Lake Cichlid Fishes via Non-Parallel Routes." *Nature Communications* 5 (October): 5168.

Ewens, Warren J. 2012. *Mathematical Population Genetics 1: Theoretical Introduction*.

Springer Science & Business Media.
Fisher, R. A. 1999. *The Genetical Theory of Natural Selection: A Complete Variorum Edition*. Oxford University Press.
Fox, Rebecca J., Jennifer M. Donelson, Celia Schunter, Timothy Ravasi, and Juan D. Gaitán-Espitia. 2019. "Beyond Buying Time: The Role of Plasticity in Phenotypic Adaptation to Rapid Environmental Change." *Philosophical Transactions of the Royal Society of London. Series B, Biological Sciences* 374 (1768): 20180174.
Garland, Theodore, Jr, Cynthia J. Downs, and Anthony R. Ives. 2022. "Trade-Offs (and Constraints) in Organismal Biology." *Physiological and Biochemical Zoology: PBZ* 95 (1): 82–112.
Gonzalez, Andrew, and Graham Bell. 2013. "Evolutionary Rescue and Adaptation to Abrupt Environmental Change Depends upon the History of Stress." *Philosophical Transactions of the Royal Society of London. Series B, Biological Sciences* 368 (1610): 20120079.
Gordo, Isabel, Lilia Perfeito, and Ana Sousa. 2011. "Fitness Effects of Mutations in Bacteria." *Journal of Molecular Microbiology and Biotechnology* 21 (1-2): 20–35.
Hamblin, M. T., and A. Di Rienzo. 2000. "Detection of the Signature of Natural Selection in Humans: Evidence from the Duffy Blood Group Locus." *American Journal of Human Genetics* 66 (5): 1669–79.
Harris, Nicholas, Marcus Bachler, Vitor Costa, Mehdi Mollapour, Pedro Moradas-Ferreira, and Peter W. Piper. 2005. "Overexpressed Sod1p Acts Either to Reduce or to Increase the Lifespans and Stress Resistance of Yeast, Depending on Whether It Is Cu(2+)-Deficient or an Active Cu,Zn-Superoxide Dismutase." *Aging Cell* 4 (1): 41–52.
Hawkins, Nichola J., Chris Bass, Andrea Dixon, and Paul Neve. 2019. "The Evolutionary Origins of Pesticide Resistance." *Biological Reviews of the Cambridge Philosophical Society* 94 (1): 135–55.
Hendry, Andrew P., Kiyoko M. Gotanda, and Erik I. Svensson. 2017. "Human Influences on Evolution, and the Ecological and Societal Consequences." *Philosophical Transactions of the Royal Society of London. Series B, Biological Sciences* 372 (1712). https://doi.org/10.1098/rstb.2016.0028.
Hohmann, Stefan. 2002. "Osmotic Stress Signaling and Osmoadaptation in Yeasts." *Microbiology and Molecular Biology Reviews: MMBR* 66 (2): 300–372.
Huang, Weini, Arne Traulsen, Benjamin Werner, Teppo Hiltunen, and Lutz Becks. 2017. "Dynamical Trade-Offs Arise from Antagonistic Coevolution and Decrease Intraspecific Diversity." *Nature Communications* 8 (1): 2059.
Jani, Divyang, Sheila Lutz, Neil J. Marshall, Tamás Fischer, Alwin Köhler, Andrew M. Ellisdon, Ed Hurt, and Murray Stewart. 2009. "Sus1, Cdc31, and the Sac3 CID Region Form a Conserved Interaction Platform That Promotes Nuclear Pore Association and mRNA Export." *Molecular Cell* 33 (6): 727–37.
Jarolim, Stefanie, Anita Ayer, Bethany Pillay, Allison C. Gee, Alex Phrakaysone, Gabriel G. Perrone, Michael Breitenbach, and Ian W. Dawes. 2013. "Saccharomyces Cerevisiae Genes Involved in Survival of Heat Shock." *G3* 3 (12): 2321–33.
Johnson, Milo S., Shreyas Gopalakrishnan, Juhee Goyal, Megan E. Dillingham, Christopher W. Bakerlee, Parris T. Humphrey, Tanush Jagdish, et al. 2021. "Phenotypic and Molecular Evolution across 10,000 Generations in Laboratory Budding Yeast Populations." *eLife* 10 (January). https://doi.org/10.7554/eLife.63910.

Jorgensen, Paul, Joy L. Nishikawa, Bobby-Joe Breitkreutz, and Mike Tyers. 2002. "Systematic Identification of Pathways That Couple Cell Growth and Division in Yeast." *Science* 297 (5580): 395–400.

Kent, David G., and Anthony R. Green. 2017. "Order Matters: The Order of Somatic Mutations Influences Cancer Evolution." *Cold Spring Harbor Perspectives in Medicine* 7 (4). https://doi.org/10.1101/cshperspect.a027060.

Kimura, Motoo. 1983. *The Neutral Theory of Molecular Evolution*. Cambridge University Press.

Konečná, Veronika, Sian Bray, Jakub Vlček, Magdalena Bohutínská, Doubravka Požárová, Rimjhim Roy Choudhury, Anita Bollmann-Giolai, et al. 2021. "Parallel Adaptation in Autopolyploid Arabidopsis Arenosa Is Dominated by Repeated Recruitment of Shared Alleles." *Nature Communications* 12 (1): 4979.

Kram, Karin E., Christopher Geiger, Wazim Mohammed Ismail, Heewook Lee, Haixu Tang, Patricia L. Foster, and Steven E. Finkel. 2017. "Adaptation of to Long-Term Serial Passage in Complex Medium: Evidence of Parallel Evolution." *mSystems* 2 (2). https://doi.org/10.1128/mSystems.00192-16.

Kryazhimskiy, Sergey, Daniel P. Rice, Elizabeth R. Jerison, and Michael M. Desai. 2014. "Microbial Evolution. Global Epistasis Makes Adaptation Predictable despite Sequence-Level Stochasticity." *Science* 344 (6191): 1519–22.

Lang, Gregory I., and Andrew W. Murray. 2008. "Estimating the per-Base-Pair Mutation Rate in the Yeast Saccharomyces Cerevisiae." *Genetics* 178 (1): 67–82.

Lässig, Michael, Ville Mustonen, and Aleksandra M. Walczak. 2017. "Predicting Evolution." *Nature Ecology & Evolution* 1 (3): 77.

Lindberg, Rasmus T., and Sinéad Collins. 2020. "Quality-Quantity Trade-Offs Drive Functional Trait Evolution in a Model Microalgal 'Climate Change Winner.'" *Ecology Letters* 23 (5): 780–90.

Lynch, Michael, Way Sung, Krystalynne Morris, Nicole Coffey, Christian R. Landry, Erik B. Dopman, W. Joseph Dickinson, et al. 2008. "A Genome-Wide View of the Spectrum of Spontaneous Mutations in Yeast." *Proceedings of the National Academy of Sciences of the United States of America* 105 (27): 9272–77.

McGee, Lindsey W., Andrew M. Sackman, Anneliese J. Morrison, Jessica Pierce, Jeremy Anisman, and Darin R. Rokyta. 2016. "Synergistic Pleiotropy Overrides the Costs of Complexity in Viral Adaptation." *Genetics* 202 (1): 285–95.

McKenna, Aaron, Matthew Hanna, Eric Banks, Andrey Sivachenko, Kristian Cibulskis, Andrew Kernytsky, Kiran Garimella, et al. 2010. "The Genome Analysis Toolkit: A MapReduce Framework for Analyzing next-Generation DNA Sequencing Data." *Genome Research* 20 (9): 1297–1303.

Moriya, H., Y. Shimizu-Yoshida, A. Omori, S. Iwashita, M. Katoh, and A. Sakai. 2001. "Yak1p, a DYRK Family Kinase, Translocates to the Nucleus and Phosphorylates Yeast Pop2p in Response to a Glucose Signal." *Genes & Development* 15 (10): 1217–28.

Nair, Shalini, Denae Nash, Daniel Sudimack, Anchalee Jaidee, Marion Barends, Anne-Catrin Uhlemann, Sanjeev Krishna, François Nosten, and Tim J. C. Anderson. 2007. "Recurrent Gene Amplification and Soft Selective Sweeps during Evolution of Multidrug Resistance in Malaria Parasites." *Molecular Biology and Evolution* 24 (2): 562–73.

Orr, H. Allen. 1998. "THE POPULATION GENETICS OF ADAPTATION: THE DISTRIBUTION OF FACTORS FIXED DURING ADAPTIVE EVOLUTION." *Evolution; International Journal*

of Organic Evolution 52 (4): 935–49.
Orr, James A., Pepijn Luijckx, Jean-François Arnoldi, Andrew L. Jackson, and Jeremy J. Piggott. 2022. "Rapid Evolution Generates Synergism between Multiple Stressors: Linking Theory and an Evolution Experiment." *Global Change Biology* 28 (5): 1740–52.
Orsini, Luisa, Katina I. Spanier, and Luc DE Meester. 2012. "Genomic Signature of Natural and Anthropogenic Stress in Wild Populations of the Waterflea Daphnia Magna: Validation in Space, Time and Experimental Evolution." *Molecular Ecology* 21 (9): 2160–75.
Pennings, Pleuni S., and Joachim Hermisson. 2006. "Soft Sweeps III: The Signature of Positive Selection from Recurrent Mutation." *PLoS Genetics* 2 (12): e186.
Pennings, Pleuni S., Sergey Kryazhimskiy, and John Wakeley. 2014. "Loss and Recovery of Genetic Diversity in Adapting Populations of HIV." *PLoS Genetics* 10 (1): e1004000.
Piper, P. W. 1995. "The Heat Shock and Ethanol Stress Responses of Yeast Exhibit Extensive Similarity and Functional Overlap." *FEMS Microbiology Letters* 134 (2-3): 121–27.
Pockrandt, Christopher, Mai Alzamel, Costas S. Iliopoulos, and Knut Reinert. 2020. "GenMap: Ultra-Fast Computation of Genome Mappability." *Bioinformatics* 36 (12): 3687–92.
Ribeiro, Gabriela Fior, Eszter Denes, Helen Heaney, and Delma S. Childers. 2022. "What 'Omics Can Tell Us about Antifungal Adaptation." *FEMS Yeast Research* 21 (8). https://doi.org/10.1093/femsyr/foab070.
Roff, D. A., and D. J. Fairbairn. 2007. "The Evolution of Trade-Offs: Where Are We?" *Journal of Evolutionary Biology* 20 (2): 433–47.
Roff, and Roff. 2000. "Trade-Offs between Growth and Reproduction: An Analysis of the Quantitative Genetic Evidence." *Journal of Evolutionary Biology*. https://doi.org/10.1046/j.1420-9101.2000.00186.x.
Schlötterer, Christian. 2023. "How Predictable Is Adaptation from Standing Genetic Variation? Experimental Evolution in Highlights the Central Role of Redundancy and Linkage Disequilibrium." *Philosophical Transactions of the Royal Society of London. Series B, Biological Sciences* 378 (1877): 20220046.
Shim, J., A. P. Newman, and S. Ferro-Novick. 1991. "The BOS1 Gene Encodes an Essential 27-kD Putative Membrane Protein That Is Required for Vesicular Transport from the ER to the Golgi Complex in Yeast." *The Journal of Cell Biology* 113 (1): 55–64.
Shoval, O., H. Sheftel, G. Shinar, Y. Hart, O. Ramote, A. Mayo, E. Dekel, K. Kavanagh, and U. Alon. 2012. "Evolutionary Trade-Offs, Pareto Optimality, and the Geometry of Phenotype Space." *Science* 336 (6085): 1157–60.
Silva, G. S., L. Zuravski, M. M. M. F. Duarte, M. M. Machado, and L. F. S. Oliveira. 2019. "Fluconazole Induces Genotoxicity in Cultured Human Peripheral Blood Mononuclear Cells via Immunomodulation of TNF-α, IL-6, and IL-10: New Challenges for Safe Therapeutic Regimens." *Immunopharmacology and Immunotoxicology* 41 (1): 123–29.
Sommer, Lea M., Helle K. Johansen, and Søren Molin. 2020. "Antibiotic Resistance in and Adaptation to Complex Dynamic Environments." *Microbial Genomics* 6 (5). https://doi.org/10.1099/mgen.0.000370.
Sopko, Richelle, Dongqing Huang, Nicolle Preston, Gordon Chua, Balázs Papp, Kimberly Kafadar, Mike Snyder, et al. 2006. "Mapping Pathways and Phenotypes by Systematic Gene Overexpression." *Molecular Cell* 21 (3): 319–30.
Spampinato, Claudia, and Darío Leonardi. 2013. "Candida Infections, Causes, Targets, and

Resistance Mechanisms: Traditional and Alternative Antifungal Agents." *BioMed Research International* 2013 (June): 204237.
Stajic, Dragan, Lília Perfeito, and Lars E. T. Jansen. 2019. "Epigenetic Gene Silencing Alters the Mechanisms and Rate of Evolutionary Adaptation." *Nature Ecology & Evolution* 3 (3): 491–98.
Sun, Liu-Liu, Hao Li, Tian-Hua Yan, Yong-Bing Cao, Yuan-Ying Jiang, and Feng Yang. 2023. "Aneuploidy Enables Cross-Tolerance to Unrelated Antifungal Drugs in." *Frontiers in Microbiology* 14 (April): 1137083.
Szamecz, Béla, Gábor Boross, Dorottya Kalapis, Károly Kovács, Gergely Fekete, Zoltán Farkas, Viktória Lázár, et al. 2014. "The Genomic Landscape of Compensatory Evolution." *PLoS Biology* 12 (8): e1001935.
Szklarczyk, Damian, Rebecca Kirsch, Mikaela Koutrouli, Katerina Nastou, Farrokh Mehryary, Radja Hachilif, Annika L. Gable, et al. 2023. "The STRING Database in 2023: Protein-Protein Association Networks and Functional Enrichment Analyses for Any Sequenced Genome of Interest." *Nucleic Acids Research* 51 (D1): D638–46.
Tenaillon, O. 2014. "The Utility of Fisher's Geometric Model in Evolutionary Genetics." *Annual Review of Ecology, Evolution, and Systematics* 45 (November): 179–201.
Vandenkoornhuyse, Philippe, Alexis Dufresne, Achim Quaiser, Gwenola Gouesbet, Françoise Binet, André-Jean Francez, Stéphane Mahé, Myriam Bormans, Yvan Lagadeuc, and Ivan Couée. 2010. "Integration of Molecular Functions at the Ecosystemic Level: Breakthroughs and Future Goals of Environmental Genomics and Post-Genomics." *Ecology Letters* 13 (6): 776–91.
Vázquez-García, Ignacio, Francisco Salinas, Jing Li, Andrej Fischer, Benjamin Barré, Johan Hallin, Anders Bergström, et al. 2017. "Clonal Heterogeneity Influences the Fate of New Adaptive Mutations." *Cell Reports* 21 (3): 732–44.
Vincent, Benjamin Matteson, Alex Kelvin Lancaster, Ruth Scherz-Shouval, Luke Whitesell, and Susan Lindquist. 2013. "Fitness Trade-Offs Restrict the Evolution of Resistance to Amphotericin B." *PLoS Biology* 11 (10): e1001692.
Watanabe, Machika, Daisuke Watanabe, Satoru Nogami, Shinichi Morishita, and Yoshikazu Ohya. 2009. "Comprehensive and Quantitative Analysis of Yeast Deletion Mutants Defective in Apical and Isotropic Bud Growth." *Current Genetics* 55 (4): 365–80.
Wei, Xinzhu, and Jianzhi Zhang. 2019. "Patterns and Mechanisms of Diminishing Returns from Beneficial Mutations." *Molecular Biology and Evolution* 36 (5): 1008–21.
Wieland, J., A. M. Nitsche, J. Strayle, H. Steiner, and H. K. Rudolph. 1995. "The PMR2 Gene Cluster Encodes Functionally Distinct Isoforms of a Putative Na+ Pump in the Yeast Plasma Membrane." *The EMBO Journal* 14 (16): 3870–82.
Wiser, Michael J., Noah Ribeck, and Richard E. Lenski. 2013. "Long-Term Dynamics of Adaptation in Asexual Populations." *Science* 342 (6164): 1364–67.
Yüzbaşioğlu, Deniz, Fatma Unal, Serkan Yilmaz, Hüseyin Aksoy, and Mustafa Celik. 2008. "Genotoxicity Testing of Fluconazole in Vivo and in Vitro." *Mutation Research* 649 (1-2): 155–60.

Supplementary Materials

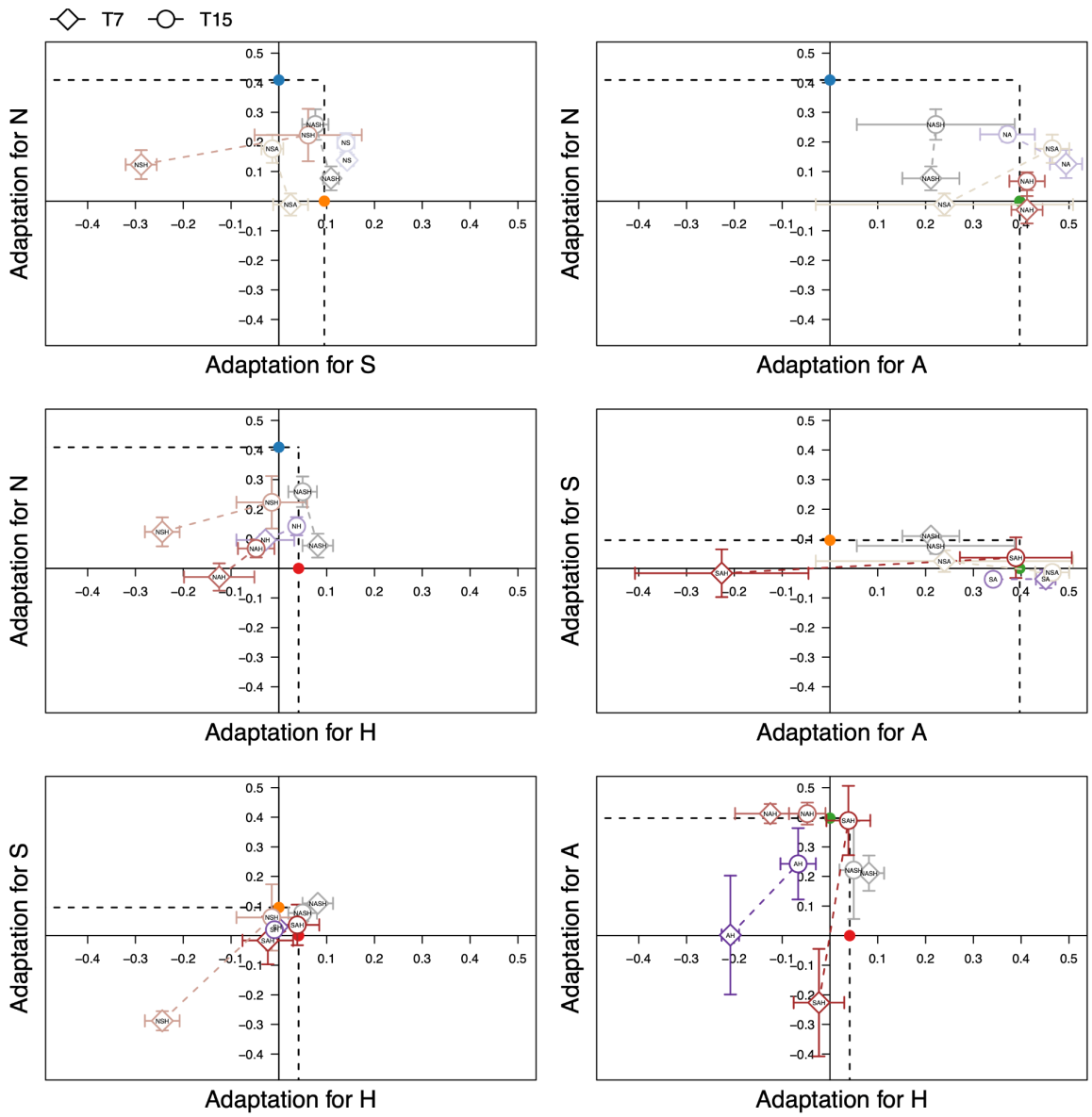

Sup Fig 1. Trade-offs in each individual component of complex environment treat- ments. Adaptation to the individual environment by the 1D specialist are shown as projections along the respective axes. Within the lower-left of the black dotted lines represents the space in which complex environments are expected to fall (i.e. less adapted in single-environments than either 1D specialist). Means are shown as diamonds or circles for T7 and T15, respectively. Standard deviations for selection coefficients are shown as bars for the respective axes.

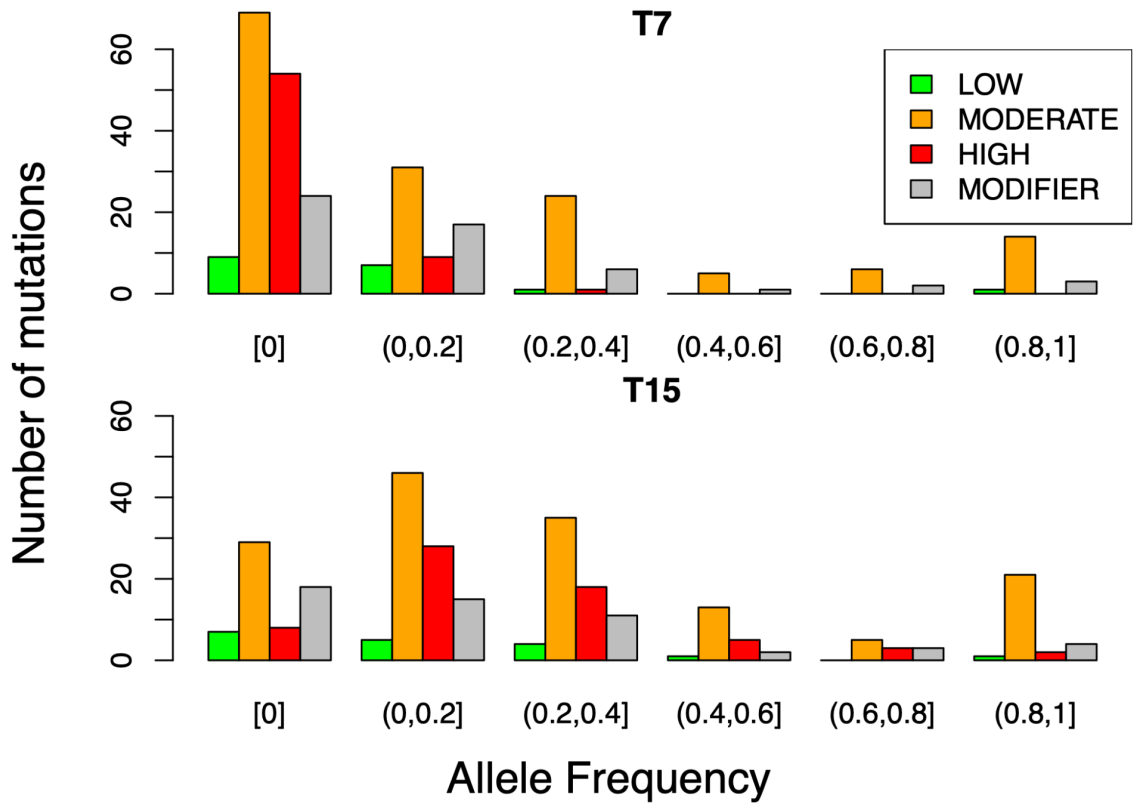

Supp. Fig 2. The number of types of mutations (SNPs and INDELs) across all evolved populations categorized by snpEff, binned by allele frequency. Mutations at AF=0 in T7 did not yet arise in any of the populations, and mutations at AF=0 in T15 are those that previously existed at T7 but were subsequently eliminated.

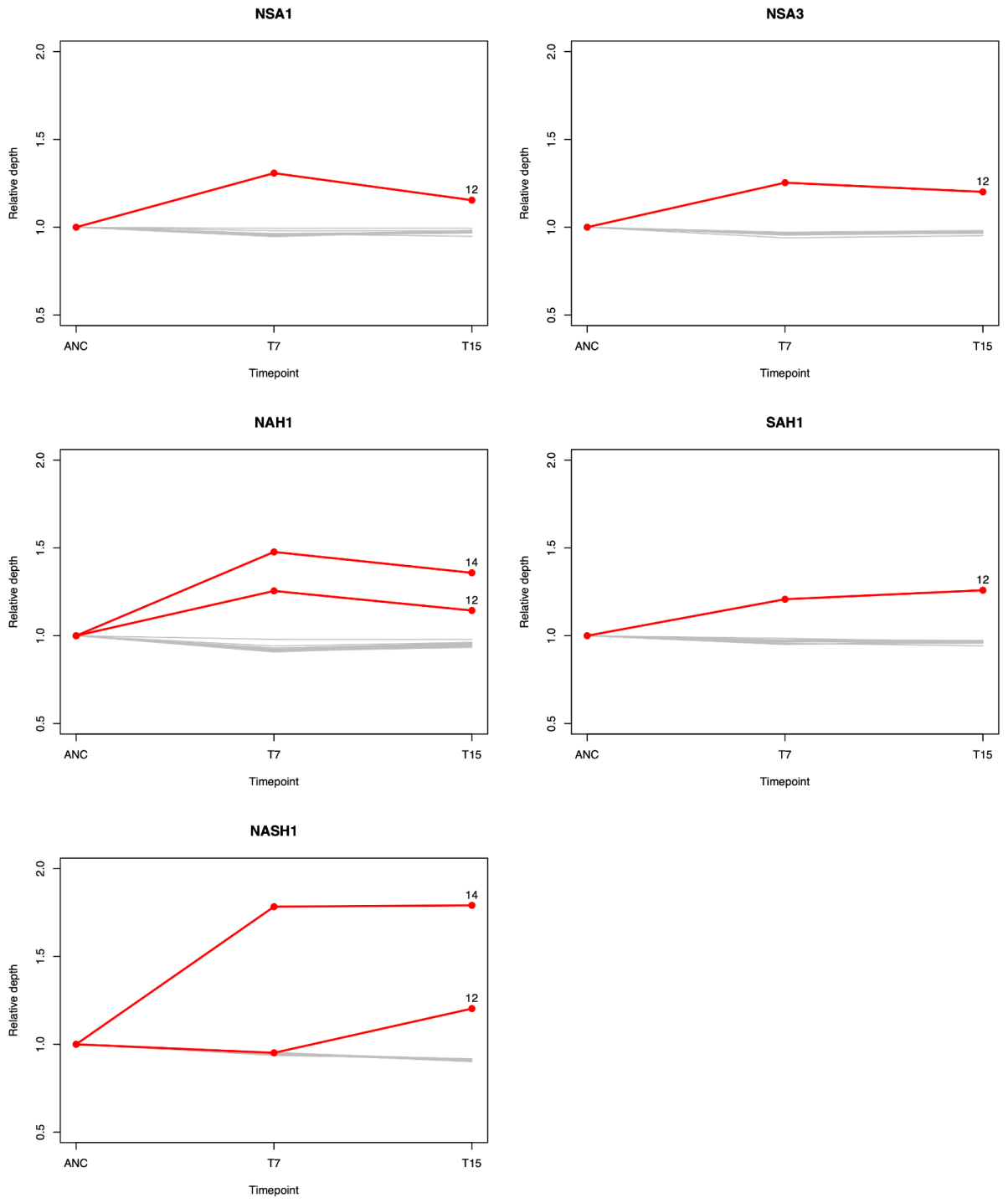

Supp. Fig 3. Aneuploidies identified in five populations. Plotted are the mean relative depths of each chromosome standardized to the ancestral population. In red are chromosomes which deviate from the ancestor relative depth by more than 20%. Putative aneuploidies are labeled with chromosome number.

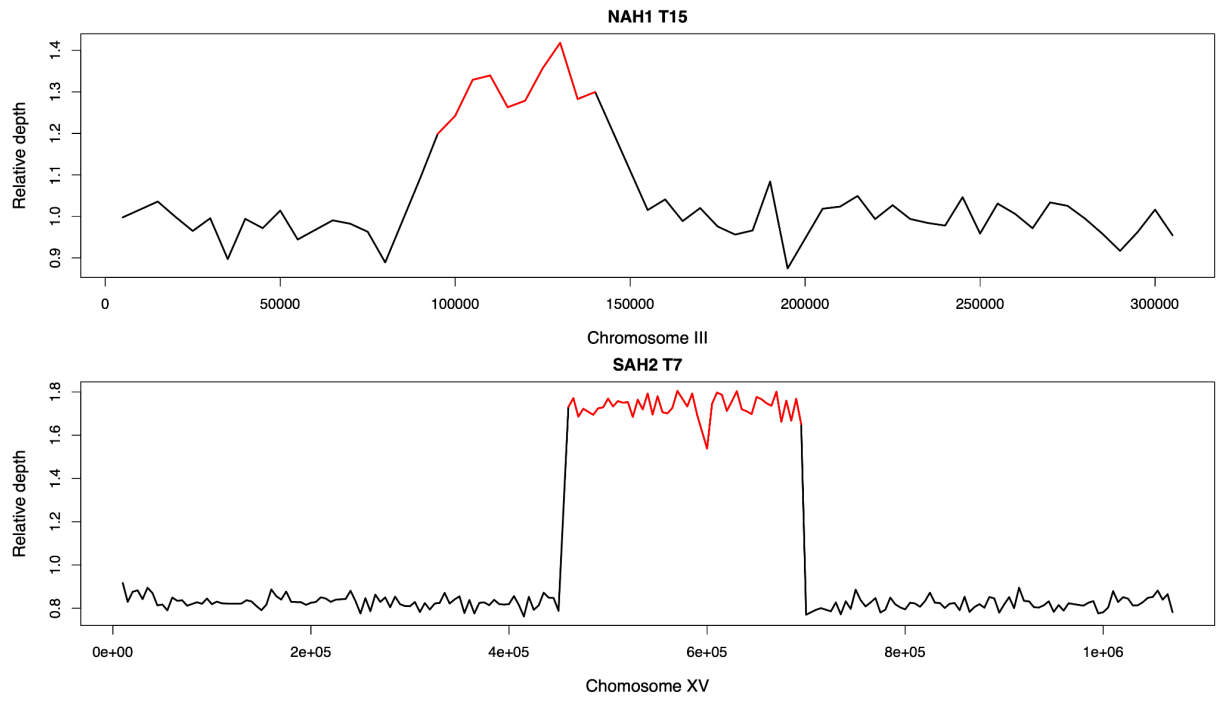

Supp. Fig 4. Copy number variants in two populations. Plotted are the mean relative depth across the genome in 5kb non-overlapping windows. In red are segments which deviate from the ancestor relative depth by more than 20%.

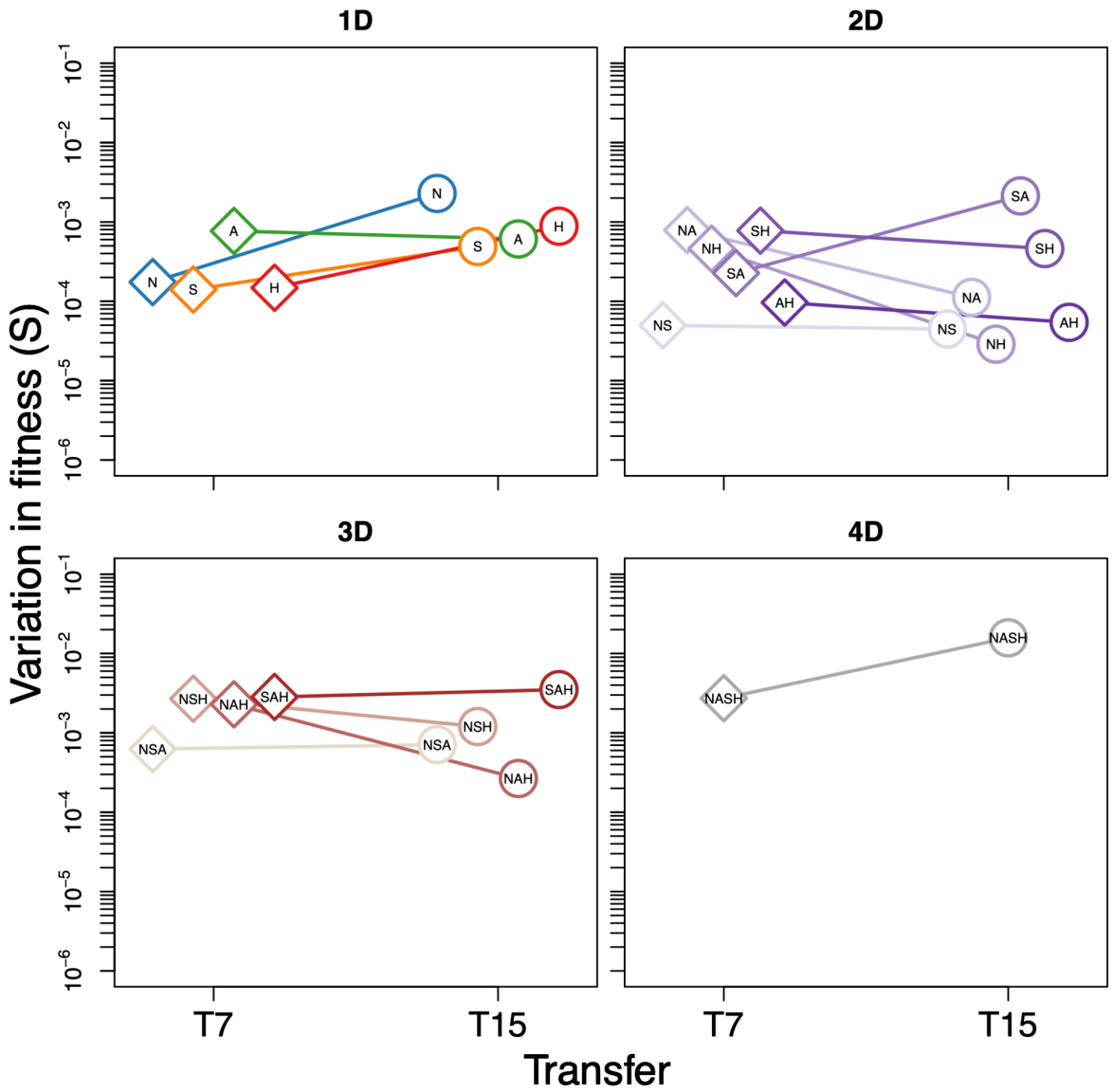

Supp. Fig. 5. Patterns of parallelism between replicates at T7 and T15 for each evolved environment. The y-axis is plotted on a log10 scale.